Zoological Journal of the Linnean Society, 2020, **XX**, 1–24. With 8 figures.

Sleeping with the enemy: unravelling the symbiotic relationships between the scale worm *Neopolynoe chondrocladiae* (Annelida: Polynoidae) and its carnivorous sponge hosts

SERGI TABOADA[1,2,3,*,†], ANA SERRA SILVA[2,4,5,†], CRISTINA DÍEZ-VIVES[2], LENKA NEAL[2], JAVIER CRISTOBO[1,6], PILAR RÍOS[1,7], JON THOMASSEN HESTETUN[8], BRETT CLARK[2], MARIA ELEONORA ROSSI[5], JUAN JUNOY[1], JOAN NAVARRO[9] and ANA RIESGO[2]

[1]*Departamento de Ciencias de la Vida, Apdo. 20, Campus Universitario, Universidad de Alcalá, 28805 Alcalá de Henares, Spain*
[2]*Life Sciences Department, The Natural History Museum, Cromwell Road, London SW7 5BD, UK*
[3]*Departamento de Biología (Zoología), Universidad Autónoma de Madrid, Facultad de Ciencias, Cantoblanco 28049, Madrid, Spain*
[4]*Division of Biosciences, University College London, Gower Street, London WC1E 6BT, UK*
[5]*School of Earth Sciences, University of Bristol, Queens Road, Bristol BS8 1RJ, UK*
[6]*Instituto Español de Oceanografía, Centro Oceanográfico de Gijón, C/ Príncipe de Asturias 70 bis, 33212 Gijón, Asturias, Spain*
[7]*Instituto Español de Oceanografía, Centro Oceanográfico de Santander, Promontorio San Martín s/n, Apdo. 240, 39080 Santander, Spain*
[8]*NORCE Environment, NORCE Norwegian Research Centre, Nygårdsgaten 112 NO-5838 Bergen, Norway*
[9]*Instituto de Ciencias del Mar CSIC, Passeig Marítim de la Barceloneta 37–49, 08003 Barcelona, Spain*

Received 13 July 2020; revised 19 September 2020; accepted for publication 14 October 2020

The North Atlantic deep-water polynoid worm *Neopolynoe chondrocladiae* is involved in an exceptional symbiotic relationship with two hosts: the carnivorous sponges *Chondrocladia robertballardi* and *Chondrocladia virgata*. While this is an obligate symbiotic relationship, its real nature is unclear. We used a multidisciplinary approach to narrow down the type of symbiotic relationship between symbiont and hosts. Molecular connectivity analyses using *COI* and 16S suggest that *N. chondrocladiae* has high potential for dispersal, connecting sites hundreds of kilometres apart, likely aided by oceanographic currents. Microbial analyses on different anatomical parts of five *Chondrocladia* species suggest that the presence of the worm in *C. robertballardi* does not affect the microbiome of the sponge. MicroCT analysis on *N. chondrocladiae* show that it has dorsally oriented parapodia, which might prevent the worm from getting trapped in the sponge. A faecal pellet recovered from the worm suggests that the polynoid feeds on the crustacean prey captured by the sponge, something corroborated by our stable isotope analysis. Light and confocal microscopy images suggest that *N. chondrocladiae* elytra produce bioluminescence. We propose that the worm might use bioluminescence as a lure for prey (increasing the food available for both the sponge and the polynoid) and thus fuelling a mutualistic relationship.

ADDITIONAL KEYWORDS: bioluminescence – confocal – microbiome – microCT – molecular connectivity – mutualism – stable isotopes – trophic relationships.

INTRODUCTION

Marine annelid polychaetes are known to engage in a multitude of symbiotic relationships, with hundreds of

*Corresponding author. E-mail: sergiotab@gmail.com
†These authors contributed equally to this work.

examples in a plethora of families (Martín & Britayev, 1998, 2018). Despite the efforts of the scientific community over the past 20 years, which have doubled the number of described symbiotic associations in polychaetes, our understanding of the interactions between these symbiotic worms and their respective hosts is still scarce and inadequate (Martín & Britayev, 1998, 2018). In their latest review on symbiotic polychaetes, Martín & Britayev (2018) highlighted that after a period when most of the reported symbiotic relationships were classified as commensal (Martín & Britayev, 1998; Britayev *et al.*, 2014), there has been an increase in the number of relationships identified as mutualistic (many of which were formerly described as commensal or parasitic), which proves the efficacy of applying new techniques and resources to the study of these symbiotic associations. However, there are still many aspects of symbiotic relationships involving polychaetes that need to be addressed in detail. Among them, for instance, is the scarce information available about behavioural observations based on living organisms (e.g. Martín *et al.*, 2015), the nature of the trophic links between host and symbiont (see: Martín & Britayev, 1998, 2018), and the phylogeographic and colonization patterns of the symbiont, limited to the best of our knowledge to just two recent contributions (Lattig *et al.*, 2017; Meca *et al.*, 2019). Difficulties in obtaining all this information are directly linked to the inherent limitations of studying marine benthic organisms, which is particularly true for deep-water species, whose collection and investigation are particularly challenging. Thus, there is a clear need to increase the information on known symbiotic relationships in polychaetes in order to provide a better understanding of their true nature.

Neopolynoe chondrocladiae (Fauvel, 1943) is a North Atlantic deep-water annelid of the family Polynoidae Kinberg, 1856 involved in an exceptional symbiotic relationship with carnivorous sponges of the genus *Chondrocladia* Thomson, 1873 (Taboada *et al.*, 2020). The symbiotic association between these organisms is noteworthy due to the fact that the symbiotic worm is a potential prey living inside its potential predator and host. Members of the genus *Chondrocladia* belong to the sponge family Cladorhizidae Dendy, 1922, and are sponge carnivores feeding primarily on small crustaceans and polychaetes (Vacelet & Duport, 2004; Vacelet, 2007). *Chondrocladia* sponges consist of several anatomical parts: roots (used to anchor the animal to the sediment), axis (which can be subdivided in multiple branches) and terminal inflatable spheres sometimes sustained by short stems (Hestetun *et al.*, 2016b). The spheres are used both for prey capture and reproduction, and maintain their turgidity thanks to a remnant aquiferous system with canals inside the main axis (Kübler & Barthel, 1999). The spheres have an adhesive surface due to the presence of velcro-like anchorate isochaelae spicules, which trap the prey; the prey is later engulfed by the sponge tissue and subsequently digested by symbiotic bacteria (Vacelet & Boury-Esnault, 1995; Vacelet & Duport, 2004; Lee *et al.*, 2012). Interestingly, two recent studies on the microbial characterization of the sponge *Chondrocladia grandis* (Verrill, 1879) showed that specific bacterial taxa were enriched in different anatomical parts, thus suggesting different microbial functional roles in sponge metabolism (Verhoeven & Dufour, 2017; Verhoeven *et al.*, 2017). Especially in the spheres, a greater abundance of Proteobacteria of the genera *Colwellia* Deming *et al.*, 1988 and *Pseudoalteromonas* Gauthier *et al.*, 1995 was found; these bacteria are known to be involved in the hydrolysis of chitin, one of the main components of crustacean exoskeletons (Verhoeven *et al.*, 2017).

In a recent study, Taboada *et al.* (2020) described morphological adaptations in both *N. chondrocladiae* and its hosts, two species of the genus *Chondrocladia*. These adaptations suggested the obligate nature of the symbiotic relationship established between the worm and the sponge. *Neopolynoe chondrocladiae* has specialized hooked chaetae in some segments, which could facilitate the attachment to, and navigation along, the branching body of the sponge host (Taboada *et al.*, 2020). These hooked chaetae have also been reported for other symbiotic polynoids (Pettibone, 1969; Martín & Britayev, 1998; Molodtsova *et al.*, 2016; Ravara & Cunha, 2016). Also, Taboada *et al.* (2020) described open galleries in the stalk of the two sponges where *N. chondrocladiae* occurs, *Chondrocladia virgata* Thomson, 1873 and *Chondrocladia robertballardi* Cristobo *et al.*, 2015. *Neopolynoe chondrocladiae* worms were found within these open galleries, which appeared not to be excavated by the polynoid, but seemed to be produced by a gradual overgrowth of the sponge to accommodate the worm (Taboada *et al.*, 2020). Similar induced galleries, commonly known as 'worm-runs', have been reported in gorgonian and hexacoral antipatharians, which are built by the host in order to provide shelter for the worm (Molodtsova & Budaeva, 2007; Britayev *et al.*, 2014). Regarding the symbiotic relationship between *N. chondrocladiae* and its two *Chondrocladia* hosts, Taboada *et al.* (2020) hypothesized that, apart from getting shelter from its host, the worm might also be getting food that sponges trap in their spheres, while the worm might be providing a benefit to the sponge by cleaning its surface and/or dissuading potential predators, as described in other examples in the literature (e.g. Martín *et al.*, 1992; Mortensen, 2001). In any case, despite the different sources of evidence provided, Taboada *et al.* (2020) hypothesized that the nature of the symbiotic relationship between the worm

and the carnivorous sponge was not clear and that further studies should be conducted to shed light on this.

In the present study, we used a combined morphological, molecular and isotopic approach to investigate phylogeographic and colonization patterns of the symbiont and also to narrow down the type of symbiotic relationship between *N. chondrocladiae* and its *Chondrocladia* hosts. Using two mitochondrial molecular markers (*COI* and 16S), we provided information about the molecular connectivity of *N. chondrocladiae* within and between sampling sites. We compared this with results obtained from *Neopolynoe acanellae* (Verrill, 1882), a closely related symbiotic polynoid associated with the alcyonacean octocoral *Acanella arbuscula* (Johnson, 1862). To determine whether there are any significant differences in the microbiome related to the presence of polynoid symbionts, we studied the microbial composition of different parts of the body of *C. robertballardi* using 16S amplicons. We compared these results to those obtained from four congeneric *Chondrocladia* species with and without symbiotic polynoids (including *Chondrocladia verticillata* Topsent, 1920, recently described to harbour other species of symbiontic polynoids; Taboada *et al.*, 2020). We then performed a thorough morphological analysis of the orientation of the parapodia of the worm using microCT scans. This helped to identify further adaptations of the polynoid to its life in symbiosis with the host. We analysed faecal pellets of the worm *N. chondrocladiae* inhabiting *C. robertballardi* and *C. virgata*, and we investigated the presence of photocytes in the elytra of *N. chondrocladiae*, *N. acanellae* and *Robertianella synophthalma* McIntosh, 1885. Finally, we used stable isotopic analysis to investigate the trophic relationships between three host–annelid associations [*A. arbuscula* and *N. acanellae*; *C. robertballardi* and *N. chondrocladiae*; *Pheronema carpenteri* (Thomson, 1869) and *Robertianella synophthalma*].

MATERIAL AND METHODS

Sample collection, preservation and identification

Neopolynoe chondrocladiae specimens were collected in association with the carnivorous sponge *C. robertballardi* from different geographic areas in the Atlantic and Indian Oceans (Fig. 1; Table 1). Specimens from the Cantabrian Sea, Avilés Canyon System (Atlantic Ocean, Spain) were collected on board the R/V *Ángeles Alvariño* (Instituto Español de Oceanografía, IEO) in June 2017, as part of the SponGES project in two sampling stations (CS-BT5 and CS-BT6; Fig. 1B; Table 1), and the R/V *Vizconde de Eza* (IEO) in July 2017, as part of the ECOMARG project (Fig. 1B; Table 1). Samples from the Gorringe Bank (Atlantic Ocean, Portugal) were collected on board the Ocean Exploration Trust R/V *Nautilus* in October 2011 as part of the NAO17 expedition (Fig. 1A; Table 1). All samples collected in the Cantabrian Sea were preserved in 96% ethanol and kept at –20 °C, while samples collected in the Gorringe Bank were preserved in 70% ethanol and kept at room temperature. All these samples were used for molecular studies (see 'DNA extraction, amplification and sequencing of *Neopolynoe* spp.' section below; Table 2). Two samples of *N. chondrocladiae* from station CS-BT6 (Fig. 1B; Table 1) were preserved in 10% formalin buffered in seawater, transferred to 70% ethanol after one day, and kept at room temperature. These samples were used for the morphological characterization of the elytra (see 'Histology, computed tomography, SEM and imaging' section below). Finally, one specimen of *N. chondrocladiae*, living in association with the carnivorous sponge *C. virgata*, was used to investigate the morphological disposition of the worm with respect to the sponge using microCT scanning (see 'Histology, computed tomography, SEM and imaging' section below). This worm was found lying on a fragment of a sponge specimen deposited at the Natural History Museum of London (NHMUK 1890.4.10.6). The presence of the worm was never reported in the description of this deposited material.

The specimens of *Neopolynoe acanellae* were always collected in association with the octocoral *A. arbuscula*. These worms were only collected from the Avilés Canyon System, from the same sampling stations as *N. chondrocladiae* (CS-BT5 and CS-BT6; Fig. 1B; Tables 1, 2) in June 2017. A total of 35 samples of *N. acanellae* were preserved in 96% ethanol and kept at –20 °C, while several samples (> 30 specimens) were preserved in formalin, as described above. As for *Robertianella synophthalma* specimens, they were always collected in association with the mud-dwelling sponge *Pheronema carpenteri* in the Cantabrian Sea (CS-BT12; Fig. 1B; Table 1), as part of the SponGES expedition on board of the R/V *Ángeles Alvariño* in 2017. A total of five specimens of *R. synophthalma* were preserved in 96% ethanol and kept at –20 °C, while two samples were preserved in formalin.

Sponges and polychaetes collected in this study were identified to the lowest taxonomic level using a number of taxonomical descriptions (Kirkegaard, 2001; Bock *et al.*, 2010; Cristobo *et al.*, 2015; Hamel *et al.*, 2015; Hestetun *et al.*, 2017). Also, all taxonomic names used were cited according to the World Register of Marine Species (http://www.marinespecies.org/).

The microbial composition (see 'Microbial community sequencing and analysis in *Chondrocladia*

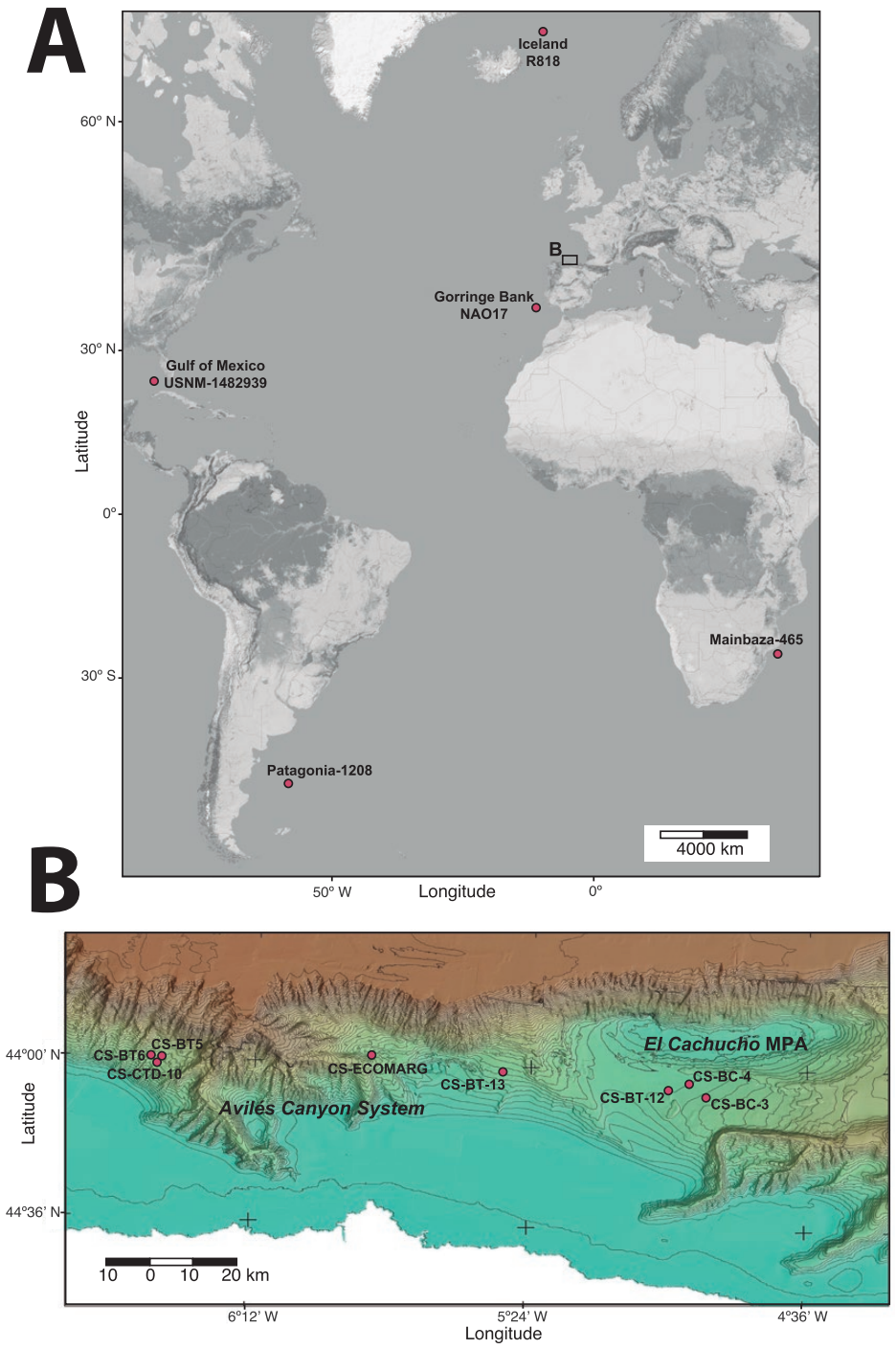

Figure 1. A, map of the sampling sites in the Atlantic and Indian Oceans. B, map of the sampling sites in the Cantabrian Sea (Atlantic Ocean). See Table 1 for details on sampling sites.

spp.' section below) was investigated for a selection of *Chondrocladia* species (Fig. 1; Tables 1, 3). These included: four specimens of *C. robertballardi* from the Avilés Canyon System (two specimens from sampling station CS-BT6, one from CS-BT5 and one from CS-ECOMARG); one specimen of *C. grandis* from Iceland, collected by trawling on board of the R/V G.O. *Sars*, within the frame of the project MAREANOS, May

Table 1. List of areas, sampling sites (CS, Cantabric Sea; GB, Gorringe Bank; Ic, Iceland, GoM, Golf of Mexico), gear used, date, coordinates, depth, and type of analyses conducted

Area	Sampling site	Gear	Date collection	Latitude	Longitude	Depth (m)	Analyses conducted
Avilés Canyon System (Cantabric Sea), Spain	CS-BT5	Beam trawl	20/06/2017	43°58.717'N	6°28.980'W	1510	Connectivity*, Microbiome†, Stable isotopes‡
Avilés Canyon System (Cantabric Sea), Spain	CS-BT6	Beam trawl	21/06/2017	43°58.866'N	6°28.622'W	1525	Connectivity*, Microbiome†, Stable isotopes‡, Microscopy
Avilés Canyon System (Cantabric Sea), Spain	CS-ECOMARG	Beam trawl	08/07/2017	43°58.884'N	5°49.484'W	1167	Connectivity*, Microbiome†, Stable isotopes‡
Avilés Canyon System (Cantabric Sea), Spain	CS-CTD10	CTD	20/06/2017	43°58.81998'N	6°28.42002'W	1522	Microbiome†
El Cachucho MPA (Cantabric Sea), Spain	CS-BC3	Box core	22/06/2017	43°55.991'N	4°53.624'W	1030	Microbiome†
El Cachucho MPA (Cantabric Sea), Spain	CS-BC4	Box core	23/06/2017	43°57.658'N	4°57.260'W	900	Microbiome†
El Cachucho MPA (Cantabric Sea), Spain	CS-BT12	Beam trawl	23/06/2017	43°57.300'N	4°58.288'W	890	Microscopy
Cantabric Sea, Spain	CS-BT13	Beam trawl	24/06/2017	43°59.286'N	5°28.567'W	1050	Stable isotopes‡
Gorringe Bank, Portugal	GB-NAO17	Beam trawl	17711/2011	36°38.9713'N	11°03.232'W	1738	Connectivity*, Stable isotopes‡
Iceland	Ic-R818	Trawling	05/05/2012	67°35.96'N	9°19.19'W	913	Microbiome†
Gulf of Mexico, USA	GoM-USNM-1482939	ROV	30/11/2017	24°39'N	83°54.6W	735	Microbiome†
Mozambique	Mainbaza-465	Chalut trawl	16/04/09	25°58.002'S	34°46.998'E	951	Microbiome†
Patagonia, Argentina	Patagonia-1208	Rock dredge	05/12/2008	45° 39.295' S	59° 39.869' W	1320	Microbiome†

*Details for samples used in the Connectivity studies are given in Table 2.
†Details for samples used in the Microbiome analyses are given in Table 3.
‡Details for samples used in the Stable isotope analyses are given in Table 4.

Table 2. Number of specimens of *Neopolynoe chondrocladiae* and *N. acanellae* used in the molecular connectivity studies

Sampling site	*N. chondrocladiae**	*N. acanellae**
CS-BT5	5 (5/5)	17 (17/17)
CS-BT6	19 (19/19)	18 (18/18)
CS-ECOMARG	3 (3/3)	—
GB-NAO17	2 (2/–)	—
Total	29 (29/27)	35 (35/35)

*In brackets, number of specimens successfully sequenced for 16S (left) and for *COI* (right). NCBI accession number of all the sequences are provided in Supporting Information, Table S1.

2012; one specimen of *C. verticillata* from the Gulf of Mexico, deposited at the Smithsonian National Museum of Natural History (USNM-1482939), November 2017; one *Chondrocladia* sp. from Mozambique, collected using a chalut trawl on board the R/V *Vizconde de Eza*, within the frame of the project MAINBAZA, April 2009; and one *Chondrocladia* sp. from Argentina, collected by rock dredged on board the R/V *Miguel Oliver*, within the frame of the project ATLANTIS, December 2008. Following Verhoeven & Dufour (2017) and Verhoeven *et al.* (2017), four different body parts of the *Chondrocladia* samples were dissected where possible, including Roots, Axis, Stem (branches supporting spheres) and Sphere. In *C. robertballardi* specimens, the section of the Axis containing *N. chondrocladiae* (Table 3) was also sampled (hereafter Axis-Poly). We also analysed the microbial composition of the Avilés Canyon System. The sediment samples were collected using a boxcore in two sites – CS-BC3 and CS-BC4 – with three replicates each (Fig. 1B; Table 1), and the water samples were obtained after filtering the content of a Niskin bottle collected near the bottom of sampling station CS-CTD10 (Fig. 1B; Table 1). All samples were preserved in 96% ethanol and kept at –20 °C.

The samples used for stable isotope analyses (see 'Stable isotope analysis' section for methodology below) included (Fig. 1B; Tables 1, 4): eight specimens of *N. chondrocladiae* and nine specimens of its host, *C. robertballardi*; and three specimens of *N. acanellae* and three specimens of its host, *A. arbuscula*. In order to have reference isotopic values of potential prey consumed by the annelids and the carnivorous sponges, we also collected zooplankton near the bottom of a sampling station in the Cantabrian Sea, as part of the SponGES project (CS-BT13; Fig. 1B; Tables 1, 4). These specimens were collected from 1 to 3 m above from the seabed using a 500-µm plankton mesh attached to the photogrammetric sled *Politolana* during one of its dives (approx. 1 h). Zooplankton samples included a range of species of crustaceans (copepods, ostracods, amphipods and cumaceans) and chaetognaths. All these organisms, especially the copepods, are among the most common prey of carnivorous sponges (Vacelet & Duport, 2004). All the samples used for stable isotope analyses were preserved in 96% ethanol and kept at –20 °C.

DNA EXTRACTION, AMPLIFICATION AND SEQUENCING OF *NEOPOLYNOE* SPP.

We performed DNA extraction of the polynoid samples using DNeasy Blood and Tissue kit (QIAGEN, Germany), following the manufacturer's protocol, except for the final elution step, where the elution buffer was warmed to 56 °C and two 75-µL buffer washes were performed. Extraction of sponge DNA was done using the E.Z.N.A. Soil DNA kit (Omega Biotek, Inc., USA), following the manufacturer's protocol with the addition of an initial 10-min vortexing in the disruptor tubes, and the final elution used 75 µL of buffer. DNA concentration of the eluted samples was quantified using NanoDrop 8000 (Thermo Fisher Scientific, USA).

We then amplified gene fragments of cytochrome *c* oxydase subunit I (*COI*) and 16S rRNA (16S) in specimens of the two *Neopolynoe* species. Primer pairs and polymerase chain reaction (PCR) programmes were as follows: for *COI* the primer pair consisted of LCO 1490 and HCO 2198 (Folmer *et al.*, 1994), and the PCR programme was 95 °C/5 min, (95 °C/1 min, 58 °C/1 min, 72 °C/1 min) × 38 cycles, 72 °C/10 min; and 16S was amplified using the arL/brH primer pair (Palumbi, 1996), and the PCR programme was 94 °C/5 min, (94 °C/1 min, 55 °C/45 s, 68 °C/45 s) × 38 cycles, 68 °C/10 min.

DNA markers were amplified in 12.5-µL reactions using 10.5 µL of VWR Red Taq DNA Polymerase 1.1× Master Mix (VWR International bvba/sprl, Belgium), 0.5 µL of the forward and reverse primers and 1 µL of DNA template, or 2 µL of PCR product for nested reactions. Polymerase chain reaction products, stained with GelRed (Biotium, USA), were visualized in a 2.5% agarose gel electrophoresis, run at 90 V for 30 min. Cleaning of the PCR products was done following the AxyPrep Mag PCR Clean-Up Protocol (Axygen Biosciences, USA) and sequencing was conducted on an ABI 3730XL DNA Analyser (Applied Biosystems, USA) at the Molecular Core Labs (Sequencing Facility) of the NHMUK, using the forward and reverse primers mentioned above. NCBI accession numbers for the 16S and *COI* sequences generated in the present study can be found in Supporting Information, Table S1.

Table 3. List of samples used in the microbial analyses. Sampling site, species or type of sample and sample collection ID is indicated for every sample

Sampling site	Species/sample type	Sample collection ID	Body part*	Sample ID-Microbial	Grouping-Microbial
CS-BT5	*C. robertballardi*	CS-BT5-551-A3	Axis	Crob_CS-BT5-551-A3-Axis	Crob_CS-BT5-551-A3
			Axis-Poly	Crob_CS-BT5-551-A3-Axis-Poly	
			Stem	Crob_CS-BT5-551-A3-Stem	
			Sphere	Crob_CS-BT5-551-A3-Sphere	
CS-BT6	*C. robertballardi*	CS-BT6-602-C	Axis	Crob_CS-BT6-602-C-Axis	Crob_CS-BT6-602-C
			Axis-Poly	Crob_CS-BT6-602-C-Axis-Poly	
			Stem	Crob_CS-BT6-602-C-Stem	
			Sphere	Crob_CS-BT6-602-C-Sphere	
CS-BT6	*C. robertballardi*	CS-BT6-602-E3	Axis	Crob_CS-BT6-602-E3-Axis	Crob_CS-BT6-602-E3
			Axis-Poly	Crob_CS-BT6-602-E3-Axis-Poly	
			Stem	Crob_CS-BT6-602-E3-Stem	
			Sphere	Crob_CS-BT6-602-E3-Sphere	
CS-ECOMARG	*C. robertballardi*	CS-ECOMARG	Axis	Crob_CS-ECOMARG-Axis	Crob_CS-ECOMARG
			Axis-Poly	Crob_CS-ECOMARG-Axis-Poly	
			Stem	Crob_CS-ECOMARG-Stem	
			Sphere	Crob_CS-ECOMARG-Sphere	
CS-CTD-10	Water sample	CS-CTD-10a	–	CS-CTD-10a	CS-CTD-10
CS-BC3	Sediment sample	CS-BC3	–	CS-BC3a	CS-BC3
				CS-BC3b	
				CS-BC3c	
CS-BC4	Sediment sample	CS-BC4	–	CS-BC4a	CS-BC4
				CS-BC4b	
				CS-BC4c	
Nw-R818	*C. grandis*	2012-106-R818-10	Roots	Cgrandis_Ic-Roots	Cgrandis_Ic
			Axis	Cgrandis_Ic-Axis	
			Stem	Cgrandis_Ic-Stem	
			Sphere	Cgrandis_Ic-Sphere	
GoM-USNM-1482939	*C. verticillata*	USNM-1482939	Roots	Cverti_GoM-Roots	Cverti_GoM
			Axis	Cverti_GoM-Axis	
			Stem	Cverti_GoM-Stem	
			Sphere	Cverti_GoM-Sphere	
Mainbaza-0308	*Chondrocladia* sp.	MAINBAZA 465	Axis	Csp_MAINB-465-Axis	Csp_Mainbaza
			Sphere	Csp_MAINB-465-Sphere	
Patagonia-1208	*Chondrocladia* sp.	PATAGONIA 1208–46	Roots	Csp_PATAGONIA-46-Roots	Csp_Patagonia-46
			Axis	Csp_PATAGONIA-46-Axis	
			Sphere	Csp_PATAGONIA-46-Sphere	
Patagonia-1208	*Chondrocladia* sp.	PATAGONIA 1208–58	Sphere	Csp_PATAGONIA-58-Sphere	Csp_Patagonia-58

Part of the body extracted is indicated for *Chondrocladia* specimens used in the study. Sample ID-Microbial and Grouping-Microbial are the names used in Figure 6. *Following Verhoeven & Dufour (2017), we separated *Chondrocladia* specimens in the following body parts: Axis, axis of the sponge; Axis-Poly, axis of the sponge where *Neopolynoe chondrocladiae* are found (only for *C. robertballardi* specimens); Roots, branching protrusions into the sediment; Sphere, inflatable spheres present at the tip of the branches; Stem, branches holding spheres branching from the main axis.

Table 4. List of samples used in the stable isotope analyses

Sampling site	Species/Taxa	Sample collection ID	Grouping-Stable isotopes	Trophic group	Potential food resources
CS-BT5	*Chondrocladia robertballardi*	CS-BT5-551-A	*C. robertballardi*	Carnivore (host of *N. chondrocladiae*)	Zooplankton (including crustaceans and annelids)
CS-BT6	*Chondrocladia robertballardi*	CS-BT6-602-A			
CS-BT6	*Chondrocladia robertballardi*	CS-BT6-602-E			
CS-ECOMARG	*Chondrocladia robertballardi*	CS-ECOMARG-A			
CS-ECOMARG	*Chondrocladia robertballardi*	CS-ECOMARG-B			
CS-ECOMARG	*Chondrocladia robertballardi*	CS-ECOMARG-C			
GB-NAO17	*Chondrocladia robertballardi*	GB-NAO17-A			
GB-NAO17	*Chondrocladia robertballardi*	GB-NAO17-B			
GB-NAO17	*Chondrocladia robertballardi*	GB-NAO17-C			
CS-BT5	*Neopolynoe chondrocladiae*	CS-BT5-551-D1	*N. chondrocladiae*	Carnivore (Symbiont of *C. robertballardi*)	Zooplankton (including crustaceans and annelids) (This study)
CS-BT6	*Neopolynoe chondrocladiae*	CS-BT6-A2			
CS-BT6	*Neopolynoe chondrocladiae*	CS-BT6-C2			
CS-ECOMARG	*Neopolynoe chondrocladiae*	CS-ECOMARG-Poly1			
CS-ECOMARG	*Neopolynoe chondrocladiae*	CS-ECOMARG-Poly2			
CS-ECOMARG	*Neopolynoe chondrocladiae*	CS-ECOMARG-Poly3			
GB-NAO17	*Neopolynoe chondrocladiae*	GB-NAO17-1204-Poly1			
GB-NAO17	*Neopolynoe chondrocladiae*	GB-NAO17-1204-Poly2			
CS-BT5	*Acanella arbuscula*	CS-BT5-555	*A. arbuscula*	Suspension feeder (host of *N. acanellae*)	Suspension feeders
CS-BT5	*Acanella arbuscula*	CS-BT5-555			
CS-BT5	*Acanella arbuscula*	CS-BT5-555			
CS-BT5	*Neopolynoe acanellae*	CS-BT5-Poly-4.1	*N. acanellae*	Carnivore (Symbiont of *A. arbuscula)*	Unkown
CS-BT5	*Neopolynoe acanellae*	CS-BT5-Poly-4.2			
CS-BT5	*Neopolynoe acanellae*	CS-BT5-Poly-4.3			
CS-BT13	Zooplankton mix	CS-BT13 Plankton	Zooplankton (Copepoda spp., Amphipoda spp., Cumacea sp., Ostracoda sp., Chaetognatha sp.)	Mixed: suspension feeders, carnivores	Bacteria and Zooplankton

Sampling site, species/taxa and sample collection ID is indicated for every sample. Samples were grouped per species/taxa. Information about trophic group (including the information about involvement in symbiotic relationships) and potential food resources is given for each species/taxa.

Haplotype networks of *Neopolynoe* spp.

Overlapping sequence fragments of *COI* and 16S were assembled separately for each marker and low-quality regions were trimmed in GENEIOUS v.10.1.3 (http://www.geneious.com; Kearse *et al.*, 2012). Consensus sequences were checked for contamination using BLAST (Altschul *et al.*, 1990), and each marker was aligned separately with the inbuilt MAFFT v.7.309 (Katoh & Standley, 2013), using the Q-INS-I option. Apart from the sequences generated here, four sequences of 16S and *COI* from *N. chondrocladiae* and *N. acanellae*, previously generated by Taboada *et al.* (2020), were also used in the analyses (see Supporting Information, Table S1).

For the haplotype network analyses, sequence alignments were manually trimmed to remove overhanging fragments, resulting in the following alignment lengths: *N. chondrocladiae*, *COI* has 471 bp and 16S has 379 bp; as for *N. acanellae*, *COI* has 491 bp and 16S has 487 bp. Haplotype networks of *COI* and 16S for *N. chondrocladiae* and *N. acanellae* were built in PopART v.1.7 (popart.otago.ac.nz; Leigh & Bryant, 2015), using the TCS algorithm (Clement *et al.*, 2000). It is important to note that for *N. chondrocladiae*, samples used in the haplotype network analysis were only grouped by sampling station; they were not also grouped by host, since *C. robertballardi* samples were fragmented (because all of them were collected by trawling) and they could not be assigned to individual specimens.

Polymorphic sites and levels of DNA polymorphism were calculated separately for each species and sampling site using the program DnaSP v.5.10.1 (Librado & Rozas, 2009), and included the number of parsimony informative characters, the number of haplotypes (*H*), the number of private haplotypes (*Hp*), the number of polymorphic sites (*Np*), the haplotype diversity (*Hd*) and the nucleotide diversity (π).

Histology, computed tomography, SEM and imaging

In order to investigate the presence of luminescent cells (i.e. photocytes) in the elytra, we prepared two formalin-preserved specimens of *N. chondrocladiae* for histological studies. A portion of the anterior section from each of the specimens (approx. ten segments) was dehydrated through an increasing ethanol series (50%, 70%, 96% and 100%), cleared in xylene and embedded in melted paraffin before cutting them into 5-µm thick sections using an Autocut Reichert-Jung microtome 2040 (R. Jung GmbH, Nubloch, Germany). After deparaffining with xylene, sections were stained with haematoxylin–eosyn, and mounted with DPX.

Histological sections, elytra and a faecal pellet from one individual of *N. chondrocladiae* were photographed using an Olympus BX43 compound microscope (www.olympus-lifescience.com; Olympus Corporation, Japan), with an Olympus UC50 camera and cellSens Standard interface v.1.16 (www.olympus-lifescience.com; Olympus Corporation, Japan). A Leica MZ6 stereomicroscope (www.leica-microsystems.com; Leica Microsystems, Germany) and the Olympus camera were used to photograph the gross morphology of the polynoids.

Elytra from specimens of *N. chondrocladiae* (CS-BT6), *N. acanellae* (CS-BT6) and *R. synopthalma* (CS-BT12), preserved in formalin, were used for confocal microscopy to identify the occurrence, disposition and arrangement of photocytes (Table 1). The emission spectrum of the elytra from *N. chondrocladiae*, *N. acanellae* and *R. synopthalma*, and the disposition of photocytes, were obtained with a Nikon Eclipse A1 Si confocal microscope (http://www.nikon.com; Nikon Corporation, Japan), at the NHMUK's imaging facilities.

A piece of the sponge *C. robertballardi* with an attached copepod from the CS-ECOMARG station was covered with gold in a BALZERS Sputter Coater SCD 004 and examined with a Jeol JSM-6610LV SEM at the Department of Scientific and Technological Resources of Oviedo University.

We performed *in situ* microCT scanning of *C. virgata* (NHMUK 1890.4.10.6) with its symbiont *N. chondrocladiae* lying on top, using a Nikon Metrology HMX ST 225 (http://www.nikon.com; Nikon Corporation, Japan), at the NHMUK imaging facilities. The purpose of this analysis was to investigate the disposition of the worm on top of the sponge and also to calculate the angle of the parapodia with respect to the body axis of the worm. The sample was stained for five days using a 50-mL solution of 5% iodine in 90% ethanol, to which an extra 50 mL of 90% ethanol was added. Scanning was performed in a Zeiss Versa 520 system with 4× optical magnification, using a Zeiss proprietary LE6 filter and exposure set to 6 s. The dataset generated during the current study is available from the corresponding author upon request. Reconstructed volumetric data were imported into VG Studio Max 2.2 (Volume Graphics Gmbh, Heidelberg, Germany), where slice stacks were rendered, reoriented and visualized in the three principal planes of sectioning (cross, horizontal and sagittal). The reconstructed data were also loaded into AVIZO 9.2. (Visualization Sciences Group, Bordeaux, France) for data segmentation, 3D visualization and volumetric measurements. Virtual sections were obtained for each chaetiger in order to measure the angle of the parapodia with respect to the body axis of the worm

along its body. Measurements were grouped into four different regions (anterior, mid-anterior, mid-posterior and posterior), with ten different measurements per region.

Stable isotope analysis

The main purpose of the stable isotope analysis was to identify the trophic relationships between the symbionts (*N. chondrocladiae* and *N. acanellae*) and their respective hosts (*C. robertballardi* and *A. arbuscula*). Isotopic analyses were performed at the Laboratory of Stable Isotopes of the Estación Biológica de Doñana (LIE-EBD, Sevilla, Spain). Encapsulated samples were combusted at 1020 °C using a continuous flow isotope-ratio mass spectrometry system, by means of a Flash HT Plus elemental analyser coupled to a Delta-V Advantage isotope ratio mass spectrometer, via a CONFLO IV interface (Thermo Fisher Scientific). The isotopic composition is reported in the conventional delta (δ) per mil notation (‰), relative to Vienna Pee Dee Belemnite (δ^{13}C) and atmospheric N_2 (δ^{15}N). Replicate assays of standards, routinely inserted within the sampling sequence, indicated analytical measurement errors of ±0.1‰ and ±0.2‰ for δ^{13}C and δ^{15}N, respectively. The standards used were EBD-23 (cow horn, internal standard), LIE-BB (whale baleen, internal standard) and LIE-PA (razorbill feathers, internal standard). These laboratory standards were previously calibrated with international standards supplied by the International Atomic Energy Agency (IAEA, Vienna). To explore the functional interpretation of the stable isotopic values, we predicted the range of expected δ^{15}N and δ^{13}C isotopic values to be found in a potential predator that consumes only zooplankton. The use of intrinsic markers, such as the stable isotopes of nitrogen (denoted as δ^{15}N) and carbon (denoted as δ^{13}C), are widely used as dietary tracers and can depict trophic position and trophic relationships between coexisting species (Boecklen *et al.*, 2011). For this prediction, the range was calculated by convex hull polygon of the isotopic values of all crustaceans sampled from the zooplankton after consumer–prey correction by an isotopic fractionation of +3.5 and +1 for δ^{15}N and δ^{13}C values, respectively (Vander Zanden & Rasmussen, 2001). This approach is based on the fact that δ^{15}N and δ^{13}C values are transformed from dietary sources to consumers in a predictable manner (Boecklen *et al.*, 2011). Nitrogen isotopic values show a predictable increase in the isotopic ratio throughout the trophic levels. Carbon isotopic values show little change with trophic transfers, but are a useful indicator of the dietary source of carbon (Vander Zanden & Rasmussen, 2001).

Microbial community sequencing and analysis in *Chondrocladia* spp.

The V4 region of the 16S rRNA gene was amplified using the universal bacterial primers 515F-Y (Parada *et al.*, 2016) and 806R (Apprill *et al.*, 2015), with the Illumina adapter overhang sequences in both primers. We used the PCRBIO HiFi Polymerase (PCR Biosystems Ltd, UK) under the following conditions: 95 °C/3 min – (95 °C/20 s – 60 °C/20 s – 72 °C/30 s) × 25 cycles – 72 °C/5 min. DNA amplification was done in duplicates and PCR products were checked in 1% agarose gel to determine the success of amplification and the relative intensity of bands. Polymerase chain reaction products were purified with AgencourtAMPure XP Beads (Beckman Coulter Inc., USA) and libraries prepared with Nextera XT DNA Library Preparation Kit (Illumina Inc., USA). An equimolar pool of DNA was generated by normalizing all samples at 4 nmol/L for the sequencing. Next generation, paired-end sequencing was performed at the NHMUK on an Illumina MiSeq device (Illumina, Inc., United States) using v3 chemistry (2 × 300 bp). The resulting amplicon sequence length was 298 bp. The raw data of the datasets presented in this study can be found in NCBI (https://www.ncbi.nlm.nih.gov/), BioProject accession number PRJNA635099, sample accession numbers SAMN15016198– SAMN15016205 and SAMN16124760–SAMN16124788 in Supporting Information, Table S1.

Raw paired reads were imported into MOTHUR v.1.41.3 and an adaptation of MiSeq SOP protocol was followed (Kozich *et al.*, 2013). Briefly, primer sequences were removed and sequence contigs built from overlapping paired reads. Sequences with > 0 N bases or with > 15 homopolymers were discarded. Unique sequences were aligned against the Silva reference dataset v.132, and poorly aligned sequences removed. Unoise3 (Callahan *et al.*, 2016) (implemented within MOTHUR) was used for denoising (i.e. error correction) of unique aligned sequences and to infer amplicon sequence variants (ASVs), allowing one mismatch per 100 bp (Oksanen *et al.*, 2019). Any singletons remaining at this stage were removed. Reference-based chimera checking was conducted using UCHIME with the Silva reference dataset and parameter minh = 0.3. Amplicon sequence variants were classified using the Silva database, with a cut-off value of 80. Amplicon sequence variants classified as eukaryotic-chloroplast-mitochondria or unknown were discarded. Description of the microbial community was done by transforming the total number of ASVs to relative abundances within each individual. The core microbiome was defined as ASVs that were present in 100% or 80% of samples at any abundance. Amplicon sequence variants generated here can be found in the

following online repository: https://doi.org/10.6084/m9.figshare.12973367.v1

Measures of ASV richness (Shannon index) were calculated using rarefied samples to the minimum sample size (i.e. 37 940 counts) in R v.3.6.1 (R Development Core Team, 2019). These metrics were compared using analyses of variance (ANOVA) among different sets of samples: (1) sponge and environment samples using a one-way analysis of variance; (2) tissue types extracted from sponges species using a two-way analysis of variance with species as a blocking factor; and (3) tissue types within *C. robertballardi* using a two-way analysis of variance with individuals as a blocking factor. Pairwise significant differences were identified using Tukey honestly significant difference (HSD).

Beta-diversity was calculated using the Bray–Curtis dissimilarity coefficient. Amplicon sequence variants were filtered by a relative abundance > 0.01%, and were log2 transformed prior to calculation of Bray–Curtis dissimilarities. Distance matrices were visualized using non-metric multidimensional scaling (nMDS) in *vegan* v.2.5–6 (De Cáceres & Legendre, 2009). Differences in microbial composition between samples and between *C. robertballardi* tissue types were detected using permutational ANOVA using 'adonis' in *vegan* and pairwise testing. Furthermore, the specific microbial families that differed in abundance between *C. robertballardi* tissue types were identified using generalized linear models in *EdgeR* v.3.26.8 (Robinson *et al.*, 2010) with individuals as blocking factors.

RESULTS

Morphological and histological analyses

Faecal pellet analysis

Out of the 29 specimens of *N. chondrocladiae* analysed, only a single faecal pellet was found in a specimen previously studied by Taboada *et al.* (2020). The pellet was found still attached to the anus and was detached to further study its composition (Fig. 2A–F). Its external appearance was shiny, resembling packed pieces of crustacean appendages (Fig. 2B). Light microscopy revealed the presence of peracarid crustacean appendages scattered within the pellet, possibly from amphipods and isopods (Fig. 2C–E), including a portion of the first pereipod of an isopod of the genus *Astacilla* Cordiner, 1793 (Fig. 2C). An aggregation of microsclere isochelae, typically found in the spheres of *C. robertballardi*, was also found in the pellet, as well as some scattered anchorate isochelae (Fig. 2E, F). In SEM micrographs of a fragment of *C. robertballardi* from the station CS-ECOMARG, we identified a recently trapped calanoid copepod, possibly from the genus *Calanus* Leach, 1819 (Fig. 2G); some of the copepod appendages were partially covered by anchorate isochelae (Fig. 2H).

Orientation of the parapodia

Stereomicroscopy showed that *N. chondrocladiae* had dorsally angled parapodia, something that was also noticed by Taboada *et al.* (2020), when sectioning the female of *N. chondrocladiae* to characterize the size and location of oocytes. We also measured the angle of the parapodia with respect to the body axis of the worm along its body in a microCT scan of a specimen of *N. chondrocladiae* living on *C. virgata* (Fig. 3). Measures were grouped in anterior (38.65° average), mid-anterior (47.03° average), mid-posterior (35.75° average) and posterior (36.59° average), showing a 37.5° orientation (ranging from 32° to 48°) for the total measures (Fig. 3B).

Histological analysis of the elytra

We observed calix-shaped photocytes arranged along the ventral side of the elytra on the histological sections of different elytra of *N. chondrocladiae*, concentrated away from the edges (Fig. 4A, B). Using confocal microscopy on the elytra of *N. chondrocladiae*, we identified brighter fluorescent cells arranged near-concentrically around the elytrophore scar and concentrated toward the centre of the elytron (Fig. 4C); the location of these cells coincided with the disposition of photocytes. Additionally, the emission spectrum of this region showed a maximum emission peak at 525 nm, and a smaller peak at 580 nm (Fig. 4C). We applied also confocal microscopy on an elytron of *N. acanellae* and identified brighter cells near the elytrophore scar but in this case restricted to one side (Fig. 4D). Finally, confocal images for an elytron of *R. synophthalma* also showed brighter cells around the elytrophore scar, although less conspicuous than for the *Neopolynoe* spp. (Fig. 4E). The emission spectrum for both *N. acanellae* and *R. synophthalma* showed a similar profile, with a maximum emission peak at 530 nm (Fig. 4D, E).

Demographic analysis and population connectivity in *Neopolynoe* spp.

The haplotype networks for *N. chondrocladiae* for 16S and *COI* showed similar star-like topologies (Fig. 5A, B). The 16S haplotype network (Fig. 5A), based on 29 samples from four sampling sites (see: Fig. 1; Table 1), recovered five haplotypes, four of which were private, with four polymorphic sites, none of which were parsimony informative. The main haplotype accounted for 86.2% of the individuals and was present in the

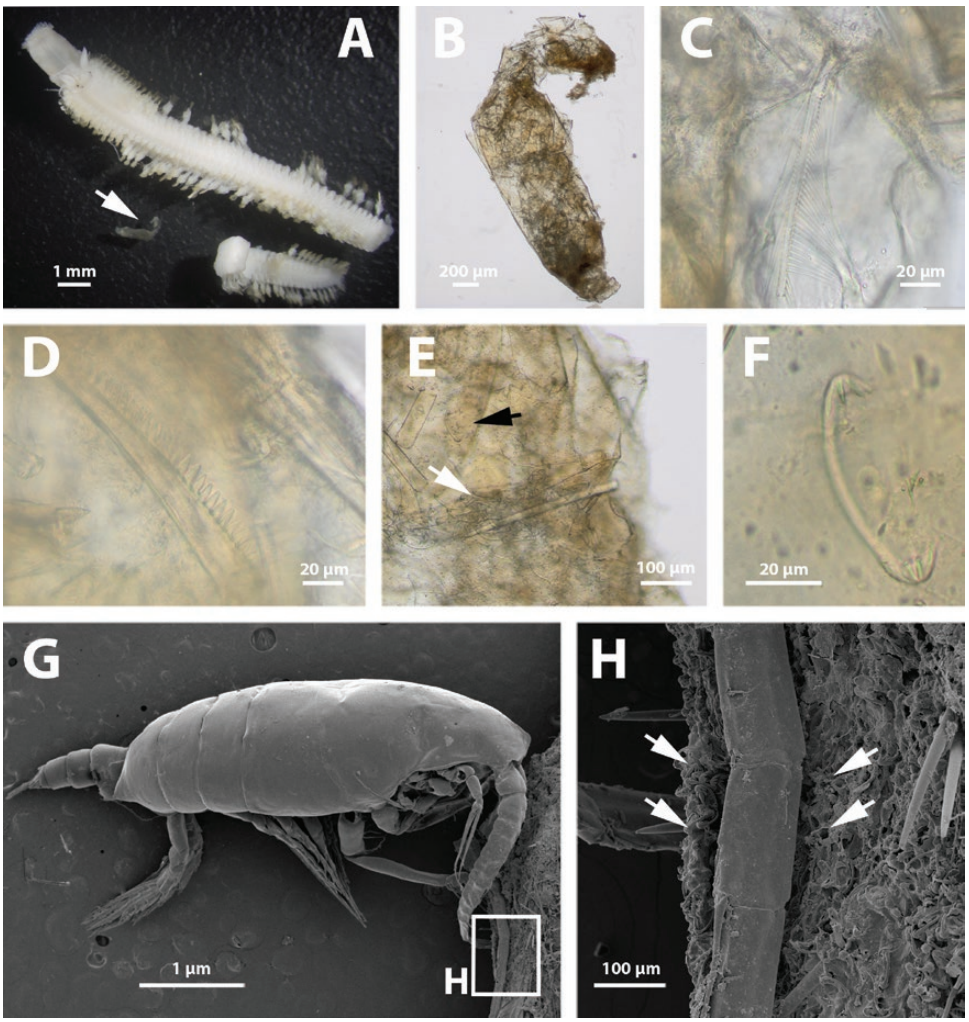

Figure 2. A–F, faecal pellet analysis of *Neopolynoe chondrocladiae* from station CS-BT6 (specimen ID CS-BT6-602-B2, light microscopy). A, general view of the polynoid; white arrow indicates the faecal pellet. B, general view of the pellet. C, detail of a pereipod fragment (possibly from the isopod genus *Astacilla*) within the pellet. D, detail of an appendage of an unidentified crustacean within the pellet. E, aggregation of microsclere isochaelae (white arrow) and scattered anchorate isochaelae (black arrow) within the pellet. F, detail of anchorate isochaela (black arrow in E). G, H, SEM micrographs of a fragment of *Chondrocladia robertballardi* (specimen ID CS-ECOMARG). G, calanoid copepod (possibly genus *Calanus*) attached to the anterior part to the axis of *C. robertballardi*. H, detail of one of the appendages of the copepod surrounded by isochaelae (white arrows).

four sampling sites. Haplotype diversity for the whole dataset was *Hd* = 0.261 ± 0.106, ranging from 0.7000 ± 0.218 in CS-BT5 to 0 in both CS-ECOMARG and GB-NAO17, while nucleotide diversity for the total individuals was π = 0.00073 ± 0.00032, ranging from 0.00211 ± 0.00080 in CS-BT5 to 0 in both CS-ECOMARG and GB-NAO17 (Table 5). The *COI* haplotype network (Fig. 5B), based on 27 samples from three populations (see: Fig. 1; Table 1), recovered six haplotypes, five of which were private, with four polymorphic sites, three of which were parsimony informative. The main haplotype accounted for 70.4% of the individuals and occurred in the three studied sampling sites. Haplotype diversity for the whole dataset was *Hd* = 0.504 ± 0.113, ranging from 0.667 ± 0.314 in CS-ECOMARG to 0 in CS-BT5, while nucleotide diversity for the total individuals was π = 0.00122 ± 0.00033, ranging from 0.00142 ± 0.00067 in CS-ECOMARG to 0 in CS-BT5 (Table 5).

Both haplotype networks for *N. acanellae* for 16S and *COI* showed similar diffuse topologies, although with a higher haplotypic diversity for *COI* (Fig. 5C, D). These haplotype networks were based on 35 individuals from two sampling stations. The 16S haplotype network

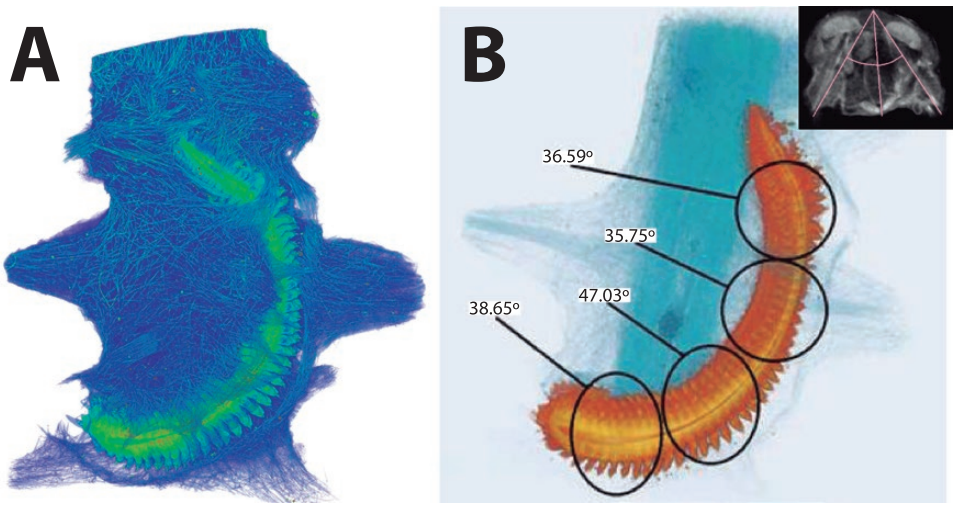

Figure 3. A, microCT scan capture of *C. virgata* (NHMUK 1890.4.10.6) and its symbiont *Neopolynoe chondrocladiae*. Full video of the scan available at https://youtu.be/I7woszSZHEk B, average angle of the parapodia with respect to the body axis of *N. chondrocladiae* along its body. Measurements were grouped in anterior, mid-anterior, mid-posterior and posterior regions. Inset showing an example of how angles were measured using virtual sections at every chaetiger.

(Fig. 5C) recovered 13 haplotypes, 11 of which were private, with 16 polymorphic sites, four of which were parsimony informative (Table 5). The main haplotype accounted for 48.6% of the individuals and 65.7% when considering the two main haplotypes, with these two haplotypes being present in the two sampling sites. Haplotype diversity for the whole dataset was Hd = 0.745 ± 0.072, with similar values in the two different sites, while nucleotide diversity for the total individuals was π = 0.00319 ± 0.00060, ranging from 0.00417 ± 0.00093 in CS-BT6 to 0.00211 ± 0.00043 in CS-BT5 (Table 5). The *COI* haplotype network (Fig. 5D) recovered 26 haplotypes, 21 of which were private, with 29 polymorphic sites, 14 of which were parsimony informative (Table 5). The main haplotype was present in 14.3% of the individuals and the rest of the haplotypes always contributed less than 10% to the whole dataset. Haplotype diversity for the whole dataset was Hd = 0.973 ± 0.016, with similar values in the two different sites, while nucleotide diversity for the total individuals was π = 0.00739 ± 0.00078, again with similar values for the two different sites (Table 5).

Microbial community analysis in *Chondrocladia* spp.

Microbial assemblage diversity and structure

The microbial community of the five *Chondrocladia* species in our study included 53 phyla, 128 genera and 307 orders, while the community of the samples collected in the surrounding environment (water and sediment) included 51 phyla, 136 genera and 311 orders. Among the *Chondrocladia* spp., the dominant phyla were Thaumarchaeota (avg: 19.4%), Proteobacteria (avg: 44.9%), Actinobacteria (avg: 11.0%), Bacteroidetes (avg: 11.5%) and Nitrospinae (avg: 7.2%) (Supporting Information, Fig. S1; Table S2). Thaumarchaeota and Proteobacteria were also dominant in the environment, but these were followed by other phyla such as Planctomycetes (avg: 13.6%), Acidobacteria (avg: 6.2%) and Rokubacteria (avg: 2.7%) (Supporting Information, Fig. S1; Table S2). At the order level, the environment was highly dominated by Nitrosopumilales (within the Thaumarchaeota, avg: 27.3%). The following orders accounted for less than 3% of mean relative abundance in the environment, and a large number of orders were condensed under the 'low abundant group' category (< 0.01% abundance) consisting of an average of 33.6% relative abundance (Supporting Information, Table S2). Conversely, in the sponge samples, several orders reached high mean relative abundances, such as Nitrosopumilales, UBA10353 marine group, Nitrospinales, Flavobacteriales, Alteromonadales, Cellvibrionales, Rhodobacterales and Oceanospirillales, and only a few orders were grouped under the low abundant category (avg: 3.1% relative abundance, Supporting Information, Table S2).

Overall, the microbiome of all five *Chondrocladia* species was similar at class level (Supporting Information, Table S2), although *C. robertballardi* had a larger proportion of orders, such as Microtrichales, Flavobacteriales and Verrucomicrobiales, and a lower abundance of Cellvibrionales and a few others (TukeyHSD, P-value < 0.05; Supporting Information, Table S2). At ASV level, the composition of the microbiome was clearly different across the

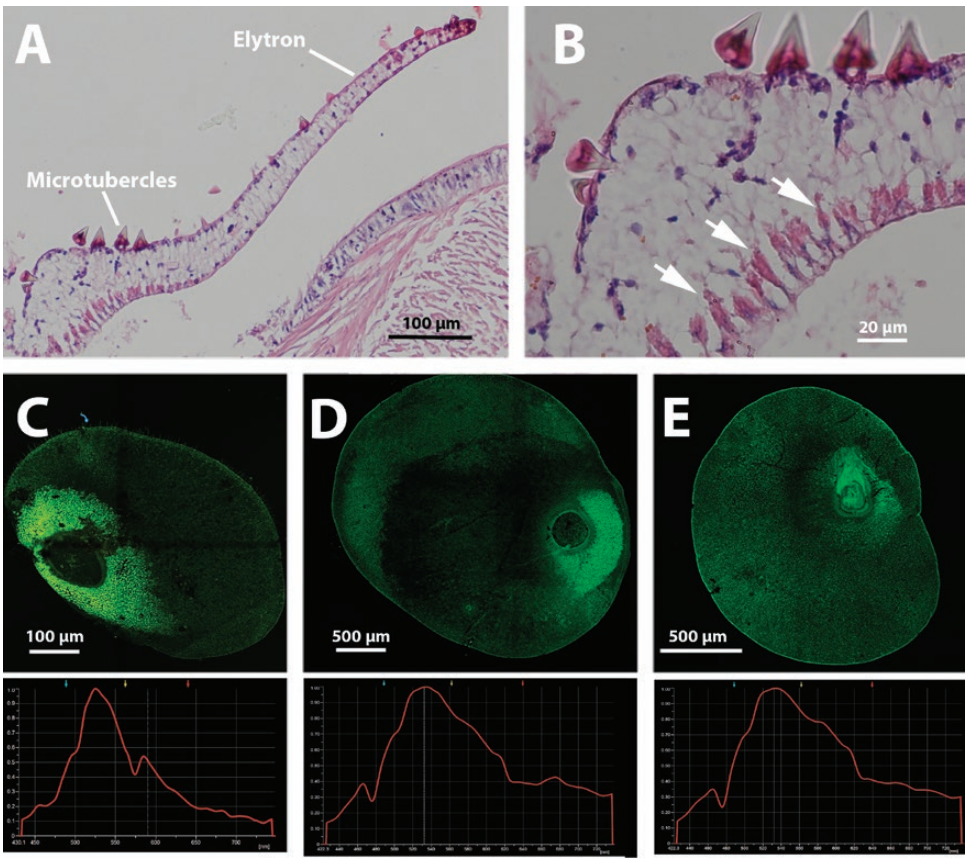

Figure 4. A, histological section of an elytron of *Neopolynoe chondrocladiae* from station CS-BT6 (specimen ID CS-BT6-602-B2) presenting some microtubercles externally. B, detail of the mid-part of the elytron showing internally calix-shaped photocytes (arrowed) arranged along the ventral side of the elytron. C, confocal microscopy picture of an elytron of *N. chondrocladiae*, ventral view. Brighter autofluorescent cells surrounding the elytrophore scar correspond to photocytes. Absorption spectrum showing a peak at 530 nm. D, confocal microscopy picture of an elytron of *Neopolynoe acanellae*, ventral view. Brighter autofluorescent cells to the right of the elytrophore scar correspond to photocytes. Absorption spectrum showing a peak at 530 nm. E, confocal microscopy picture of an elytron of *Robertianella synopththalma*, ventral view. Brighter autofluorescent cells around the elytrophore scar correspond to photocytes. Absorption spectrum showing a peak at 530 nm.

Chondrocladia spp. (Fig. 6). We obtained 19 654 ASVs for all the sponge samples, but only a small number of them accounted for most of the abundance (i.e. 20 ASVs covered a mean of 79% of relative abundance on average), except for the *Chondrocladia* sp. 'Patagonia' Root sample, where these 20 ASVs only represented 1.9% of relative abundance. The environment samples included 31 246 ASVs, with the top 20 ASVs accounting for 19.6% mean relative abundance, except for the seawater sample (0.018%). The heatmap also showed that most of the ASVs present in the sediment and seawater samples were absent or had low abundance in the sponge samples and vice versa (only 11.7% of ASVs were shared between environment and sponges), indicating a sponge-specific microbiome different to the surrounding environment (Fig. 6).

Looking at the alpha diversity, the sediment was the most diverse group, followed by the seawater, which were statistically significantly more diverse than any sponge sample (ANOVA, $P < 0.001$; Fig. 7A; Supporting Information, Table S3a). Considering only the sponge samples, differences in their global diversity (all tissues together) between species were also significant (ANOVA, $P = 0.0017$; Supporting Information, Table S3b), with *Chondrocladia* sp. 'Mainbaza' and *C. verticillata* having lower diversity than the other species (Fig. 7A). Between anatomical regions, Roots was usually the most diverse sample type and Stem the lowest, except for *C. grandis* where the Axis was more significantly diverse than Roots. Statistically, there were no significant differences among the other sample types (Fig. 7A; Supporting

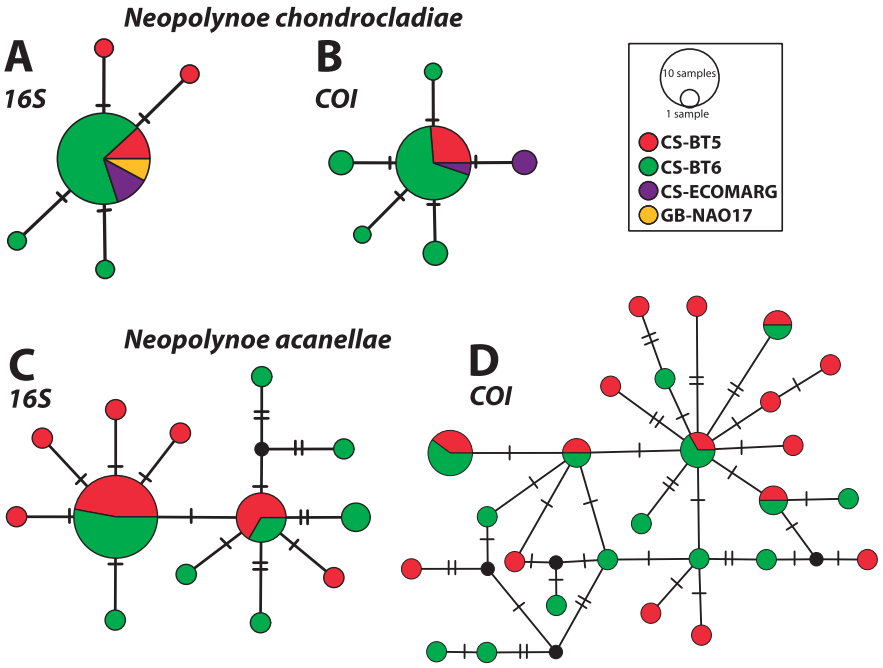

Figure 5. 16S and *COI* TCS haplotype networks for *Neopolynoe chondrocladiae* (A, B) and *Neopolynoe acanellae* (C, D), colour-coded by sampling station (see box). Each circle represents a distinct haplotype and the size is proportional to the number of individuals. Hatch marks on branches correspond to the number of mutational steps between haplotypes. Missing inferred haplotypes are in black. See Table 2 for details about number of specimens used for each species and genetic marker.

Information, Table S3b). Focusing on the four individuals of *C. robertballardi* (no Roots' samples available), diversity usually decreased from Sphere, to Stem and Axis (Fig. 7B). In three individuals, the Axis-Poly (hosting polychaetes) showed larger diversity than the Axis without polychaetes, but one individual showed the opposite trend (Fig. 7B). Statistically, individuals of *C. robertballardi* were not significantly different (P = 0.207; Supporting Information, Table S3c) and anatomical regions were only marginally different (ANOVA, P = 0.048; Supporting Information, Table S3c).

The nMDS plot of the beta diversity grouped samples by sediment, seawater or sponge species (PERMANOVA, P = 0.001; Supporting Information, Table S4a), confirming that the community of sponges is different from the environment, and that species is the most important factor determining the sponge microbiome (Fig. 7C). As expected from the previously observed differences, Roots of *Chondrocladia* sp. 'Patagonia' clustered away from any other sample (Fig. 7C). Within *C. robertballardi*, there was an effect of the sampling location (Supporting Information, Fig. S2), and after correcting for this effect, anatomical regions (i.e. Sphere, Stem and Axis/Axis-Poly) were separated by axis 1 (Fig. 7D) and were not significantly different (PERMANOVA, P = 0.084; Supporting Information, Table S4b). Pairwise comparisons showed that the differences occurred between Sphere and Axis or Axis-Poly tissues ($P < 0.1$; Supporting Information, Table S4c).

Core and specific microbiome

Sediment samples reached a strict (100% of the samples) core microbiome of 1551 ASVs, and up to 2966 ASVs were present in 80% of the samples. In *Chondrocladia* sponges there was no strict core microbiome, but we identified eight core ASVs, including 80% of samples, which represented from 1.1 to 43.6% relative abundance in different samples. These core ASVs belonged to one *Candidatus Nitrosopumilus* (Thaumarchaeota) and six Proteobacteria, including Halieaceae, Betaproteobacteria EC94, *Colwellia* and *Roseobacter* clade NAC11-7. By sponge species: *Chondrocladia* sp. 'Mainbaza' (two samples) had 125 core ASVs; *Chondrocladia* sp. 'Patagonia' (four samples) had 24 core ASVs; *C. verticillata* (four samples) had 80 core ASVs; *C. grandis* (four samples) 162 ASVs; and *C. robertballardi* (16 samples) presented a core community with 44 core ASVs, ranging from 64 to 84.5% relative abundance (Supporting Information, Table S5a).

Table 5. Haplotype diversity metrics of *Neopolynoe chondrocladiae* and *Neopolynoe acanellae* for 16S and *COI* for each sampling site

Neopolynoe chondrocladiae			**16S**			
Sampling Site	***N***	***H***	***Hp***	***Np***	***Hd***	***π***
CS-BT5	5	3	2	2	0.7000 ± 0.218	0.00211 ± 0.00080
CS-BT6	19	3	2	2	0.205 ± 0.119	0.00056 ± 0.00033
CS-ECOMARG	3	1	0	0	0	0
GB-NAO17	2	1	0	0	0	0
Total	29	5	4	4	0.261 ± 0.106	0.00073 ± 0.00032
			COI			
Sampling Site	***N***	***H***	***Hp***	***Np***	***Hd***	***π***
CS-BT5	5	1	0	0	0	0
CS-BT6	19	5	2	4	0.532 ± 0.130	0.00129 ± 0.00038
CS-ECOMARG	3	2	1	1	0.667 ± 0.314	0.00142 ± 0.00067
Total	27	6	2	5	0.504 ± 0.113	0.00122 ± 0.00033
Neopolynoe acanellae			**16S**			
Sampling Site	***N***	***H***	***Hp***	***Np***	***Hd***	***π***
CS-BT5	17	7	5	6	0.750 ± 0.92	0.00211 ± 0.00043
CS-BT6	18	8	6	11	0.752 ± 0.103	0.00417 ± 0.00093
Total	35	13	11	16	0.745 ± 0.072	0.00319 ± 0.00060
			COI			
Sampling Site	***N***	***H***	***Hp***	***Np***	***Hd***	***π***
CS-BT5	17	16	15	24	0.993 ± 0.023	0.00743 ± 0.00087
CS-BT6	18	15	10	18	0.974 ± 0.029	0.00737 ± 0.00111
Total	35	26	21	29	0.973 ± 0.016	0.00739 ± 0.00078

N, number of samples; *H*, number of haplotypes; *Hp*, number of private haplotypes; *Np*, number of polymorphic sites; *Hd*, haplotype diversity; π, nucleotide diversity.

These core ASVs in *C. robertballardi* included taxa such as *Nitrososphaeria* (Archaea), Acidimicrobiia, Bacteroidia, Planctomycetacia, Colwelliaceae, Pseudoalteromonadaceae, Cellvibrionales and Oceanospirillales (Supporting Information, Table S5a). Core ASVs were less common for the same tissue type across all five *Chondrocladia* species. Sphere samples (nine samples) shared zero core ASVs, Stem tissue (six samples) shared five core ASVs, Axis (eight samples) shared one core ASVs, and Roots (three samples) shared 65 ASVs (Supporting Information, Table S5b). Within *C. robertballardi*, the tissue types shared 107 and 114 ASVs for Axis and Axis-Poly, respectively, and 139 y 140 ASVs within Stem and Sphere, respectively (Supporting Information, Table S6).

We further investigated differences in bacterial abundance (family level) among tissue samples of *C. robertballardi* (considering 'individual' as blocking factor in EdgeR). A total of 30 families differed among any pair of tissue type (Supporting Information, Table S7). Some of these taxa included Nitrospinales, Alteromonadales (families Colwelliaceae, Pseudoalteromonadaceae), Betaproteobacteriales (family EC94), Cellvibrionales (families Halieceaceae and Spongiibacteraceae), Oceanospirillales, Gammaproteobacteria (family JBT23), Cytophagales and Verrucomicrobiales (Supporting Information, Fig. S3). Between Sphere vs. Axis or Axis-Poly there were 29 and 25 differential families (with significantly more abundance in one tissue sample than the other), respectively; and nine between Sphere and Stem, most of them presenting higher abundance in the Sphere tissue (Supporting Information, Fig. S3; Table S7). Only families Nitrospinaceae, Rhodobacteraceae, Halieaceae, Psedohongiellacea and Flammeovirgaceae showed smaller abundance in the Sphere compared to the other tissues. Stem possessed 21 families with higher abundance compared to the Axis/Axis-Poly tissues, which were

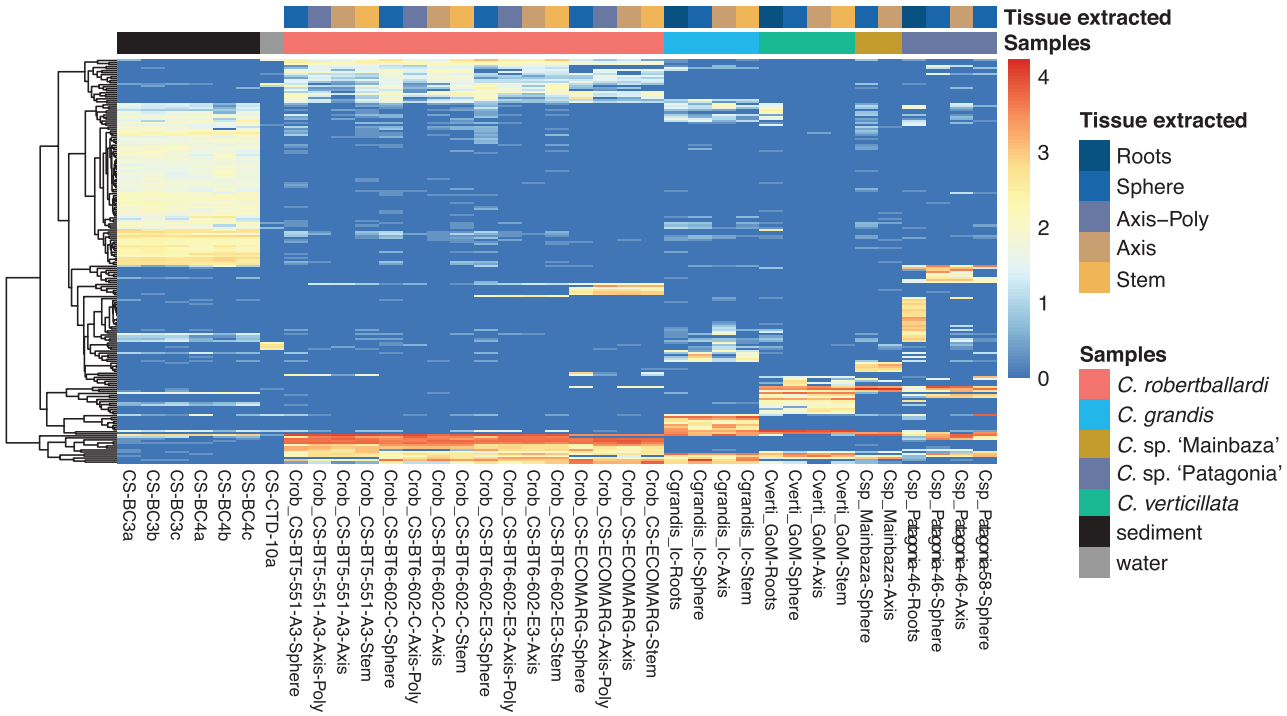

Figure 6. Heatmap showing the top 200 most abundant ASVs for each sample. The colour range (0 to 4) represents the log10 transformation of the rarefied counts.

the same as in the Sphere comparisons. Interestingly, the comparison of Axis vs. Axis-Poly revealed no differences at genus level (Supporting Information, Fig. S3; Table S7).

Stable isotope analysis

The δ^{15}N values ranged between 10.70‰ (*A. arbuscula*) and 14.61‰ (*C. robertballardi*), while for δ^{13}C, the values ranged between −4.81‰ (*A. arbuscula*) and −19.42‰ (*N. chondrocladiae*) (Fig. 8). The comparison between each host–annelid combination showed that the sponge *C. robertballardi* and the annelid *N. chondrocladiae* had similar δ^{15}N and δ^{13}C values (Fig. 8), indicating that annelid and host occupied the same trophic position. In contrast, the cnidarian *A. arbuscula* and the annelid *N. acanellae* differed in their δ^{13}C and δ^{15}N values (Fig. 8), indicating that both partners exploit different resources, with the worm occupying a higher trophic level. The predicted range of expected isotopic values to be found in a potential predator that consumes only zooplankton partially overlap with the isotopic position of the sponge *C. robertballardi* and the annelids *N. acanellae* and *N. chondrocladiae* (Fig. 8), indicating that these species could both be feeding on zooplankton.

DISCUSSION

Many different aspects of symbiotic relationships involving polychaetes are still unknown for the majority of species (Martín & Britayev, 2018). Here we describe the nature of the trophic relationship between the worm and its hosts based on multiple sources of evidence and also provide insights on the phylogeographic and colonization patterns of the symbiotic worm *N. chondrocladiae*.

Molecular connectivity and dispersal in *Neopolynoe* spp.

Demographic analysis, as inferred from the haplotype networks and demographic parameters in both *N. chondrocladiae* and *N. acanellae*, showed similar patterns for both genetic markers for each of the species separately (Fig. 5). *Neopolynoe acanellae* showed high nucleotide and haplotype diversity (i.e. genetic diversity) and a diffuse haplotype network (Fig. 5C, D). As the populations sampled were only 0.6 km away from each other, nothing can be inferred about the dispersal capabilities of the species. However, the relatively high values of genetic diversity indicate genetically diverse populations for this species. Similar results were reported for the deep-sea Mediterranean polychaete *Iphitime cuenoti*

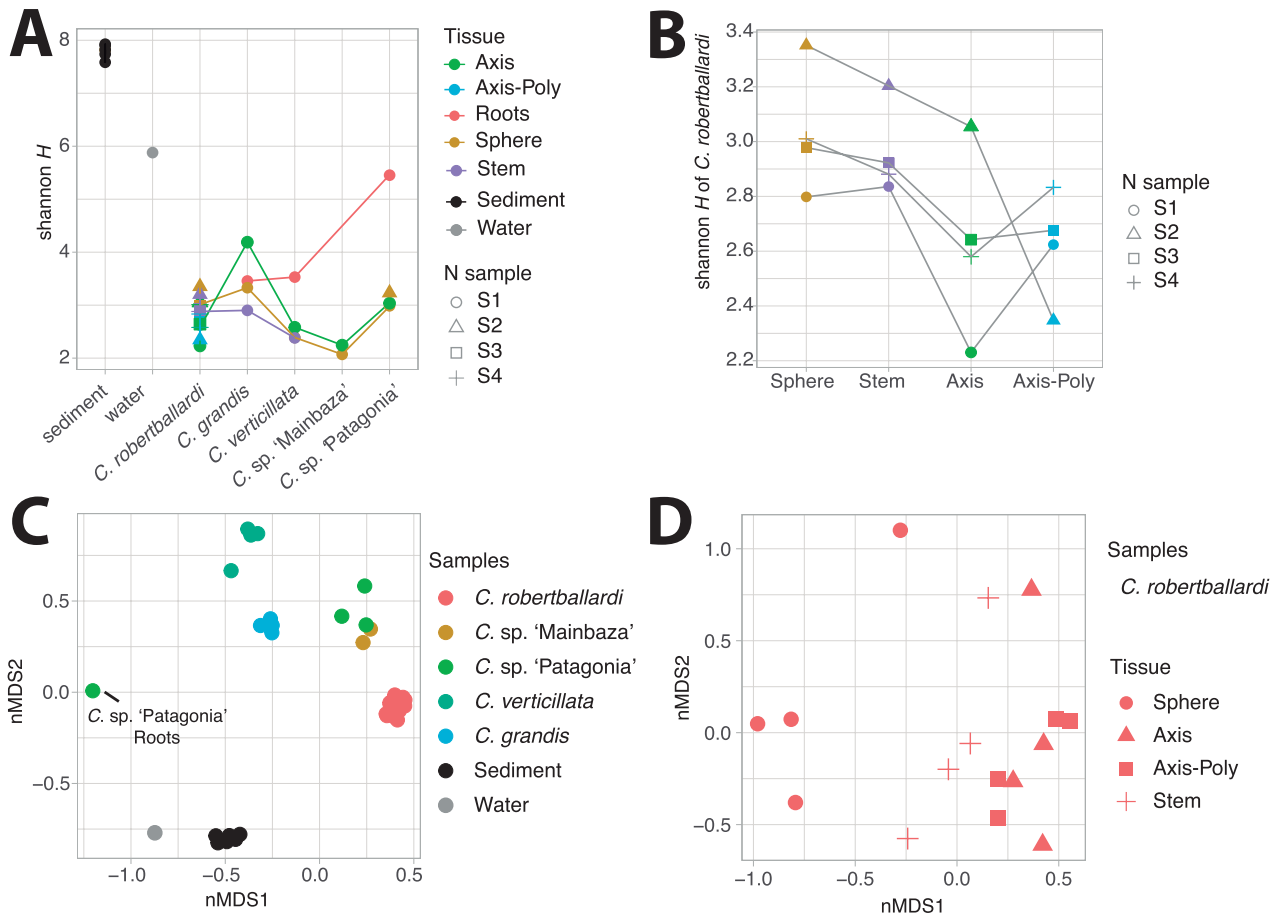

Figure 7. A, ASV richness (Shannon index) using rarefied counts for all the samples in this study. Samples are differentiated by species, tissue type and replicate. B, ASV richness (Shannon index) using rarefied counts for *Chondrocladia robertballardi*. Samples are differentiated by tissue type and replicate. C, non-metric multidimensional scaling (nMDS) ordination of microbiome similarity among samples in this study. D, nMDS ordination of microbiome similarity among samples of *C. robertballardi*, after data correction for sampling site effect.

Fauvel, 1914 (Lattig *et al.*, 2017). This symbiotic worm showed a *COI* star-like haplotype with some derived haplotypes, although in this case the sampling sites ranged hundreds of kilometres. However, results for *N. acanellae* contrasted with those recently reported for the symbiotic hesionid *Oxydromus okupa* Martín, Meca & Gil in Martín *et al.* (2017), which showed a low-diversity star-like haplotype network for 16S after analysing shallow-water specimens from two nearby sampling sites (Meca *et al.*, 2019).

Neopolynoe chondrocladiae showed less genetic diversity than *N. acanellae* and star-like haplotype networks (Fig. 5A, B). Interestingly, the predominant ancestral haplotype for 16S in *N. chondrocladiae* was shared between specimens collected in populations more than 900 km apart, which may indicate long-distance connectivity for this species. The relatively small average oocyte diameter (56.94 ± 14.89 μm) observed for *N. chondrocladiae* was assumed to be consistent with the presence of free-spawning gametes and a planktotrophic larva (Taboada *et al.*, 2020), a type of reproduction that has generally been linked with a higher dispersal ability (Giangrande, 1997; Weersing & Toonen, 2009). Oceanographic currents running northwards along the coast of Portugal to the Cantabrian Sea (González-Pola *et al.*, 2012; Llave *et al.*, 2015) might be the major dispersal avenue for *N. chondrocladiae*. This hypothesized long-distance connectivity, linking sites hundreds of kilometres away, is not at all surprising and appears to be the rule for deep-water organisms occurring at similar depths, with bathymetric ranges being the main factor explaining the genetic structure observed among deep-water populations (see: Taylor & Roterman, 2017).

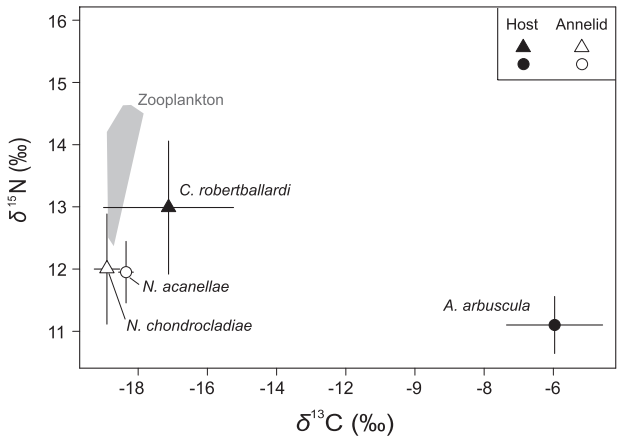

Figure 8. Stable isotopic values (mean and standard deviation of δ^{15}N and δ^{13}C) of the different hosts (*Acanella arbuscula* and *Chondrocladia robertballardi*) and annelids (*Neopolynoe acanellae* and *N. chondrocladiae*) collected in this study. Zooplankton values correspond to a mixture of species of crustaceans (copepods, ostracods, amphipods, and cumaceans) and chaetognaths.

Alternatively, sharing haplotypes between distant sampling sites may be a consequence of an ancestral polymorphism that was retained in individuals originating from a refugial population (De Jong *et al.*, 2011; Zhang *et al.*, 2014). This may have resulted in a high genetic similarity of the newly expanding populations, falsely implying extensive gene-flow (Maggs *et al.*, 2008). However, in order to test this hypothesis, larger sample sizes should be investigated and further analyses should be conducted using more informative genetic markers, such as microsatellites or single nucleotide polymorphisms (SNPs).

Intra- and interspecific differences in the microbial community of *Chondrocladia* spp. with and without polychaetes

In general, the microbiome of all *Chondrocladia* species was similar at higher taxonomic orders (except for a few orders; Supporting Information, Table S2), but was different at the ASV level (Fig. 6), congruent with the proposed microbiome host-specificity presented by Thomas *et al.* (2016). The most abundant group in *Chondrocladia* spp. was Nitrosopumilales, a relatively common group of ammonia oxidizing archaea found in deep-sea sponges (Kennedy *et al.*, 2014), that has also been reported in other carnivorous sponges (Dupont *et al.*, 2013; Hestetun *et al.*, 2016a). In terms of alpha-diversity, *Chondrocladia robertballardi* was not either the most or the least diverse species, showing relatively similar values to *C. grandis* and *C. verticillata*, which are the more closely related species (Verhoeven *et al.*, 2017).

In *Chondrocladia robertballardi*, three out of four of the Axis-Poly samples (hosting polychaetes) showed larger diversity than the Axis samples without polychaetes. These differences were not supported statistically, indicating that *N. chondrocladiae* might not be affecting the microbiome of *C. robertballardi*. However, *C. robertballardi* showed a specific microbiome for the different tissue types (i.e. Sphere, Stem, Axis/Axis-Poly), being the Sphere significantly different from the Axis tissues, and not significantly different from the Stem. In fact, Sphere and Axis samples had 30 families with different abundances, usually higher in the Sphere, but only nine families were different with the Stem (Supporting Information, Table S7). Sphere was also the tissue type with higher alpha diversity, followed by the Stem and the Axis in *C. robertballardi*, but this diversity was lower than any of the Roots' samples in the other species (Fig. 7A). Higher diversity values associated to Roots were also observed by Verhoeven *et al.* (2017) in their study on *C. grandis* when comparing the Roots to Axis and Sphere tissues. Sphere in *C. robertballardi* presented higher relative abundances of *Colwellia* and *Pseudoalteromonas*, similar to what Verhoeven *et al.* (2017) reported for *C. grandis*. These groups of bacteria are known to hydrolyse chitin, and their preferential occurrence in the spheres was suggested to be involved in prey breakdown and digestion (Verhoeven *et al.*, 2017).

The symbiotic relationship between *Neopolynoe chondrocladiae* and *Chondrocladia robertballardi*

The symbiotic association between the polynoid *N. chondrocladiae* and its sponge hosts *C. robertballardi* and *C. virgata*, was recently described by Taboada *et al.* (2020). In this paper, the authors suggested an obligate symbiotic relationship between worm and sponge, mainly based on the existence of specialized chaetae in *N. chondrocladiae* and the occurrence of open galleries in the host sponge, derived from a gradual overgrowth of the sponge, and built to accommodate the worm (Taboada *et al.*, 2020). The presence of distally hooked neuropodial chaetae in the polynoid were suggested to enable the worm to navigate the branches of its host, allowing it to reach the spicule-rich spheres where the sponge traps its prey (Taboada *et al.*, 2020). Our in-detail studies on the angle of parapodia in *N. chondrocladiae* suggest another adaptive morphological modification of the worm to the symbiotic life. We propose that the dorsally angled parapodia, apart from helping the worm to navigate along the branched body of the

sponge, may prevent the neurochaetae of the polynoid from getting trapped in the spheres, thus preventing the host from predating on its symbiont. The dorsally oriented parapodia reported in *N. chondrocladiae* have never been reported in any other *Neopolynoe* species, where neurochaetae are always directed ventrally [but see fig. 5C in Taboada *et al.* (2020)], although they have been described in *Parahololepidella greeffi* (Augener, 1918), a shallow-water polynoid symbiont of the branching antipatharian coral *Tanacetipathes* cf. *spinescens sensu* Britayev *et al.* (2014).

We obtained evidence that *N. chondrocladiae* might be feeding on prey trapped by the sponge in its spheres coming from observations of a faecal pellet from an individual living in association with *C. robertballardi*. This faecal pellet included many small crustacean remains, along with some hooked microsclere spicules, which are mainly found in the spheres of the sponge. Given that there were no clear injuries in any of the sponge specimens that we investigated, we suggest that the presence of aggregations of spicules in the faecal pellet might result from accidentally ingesting some of the spicules that get attached to the crustacean appendages when they are trapped in the spheres. Furthermore, the similar stable isotope values between the sponge host and the polynoid symbiont confirm the faecal observation, indicating that both organisms feed on similar trophic resources, probably crustaceans present in the zooplankton, thus ruling out the possibility that the worm may also be consuming the sponge. Also, as inferred by our microbial community analyses (see above), no clear evidence was found that the presence of the worm affects the composition of the microbial assemblage in the sponge.

Given the information gathered here, the nature of the symbiotic relationship between *N. chondrocladiae* and its *Chondrocladia* hosts is likely to be mutualistic, rather than parasitic. The evidence from morphological, genetic and trophic analyses with stable isotopes point to a mutualistic relationship, with benefits for both parties and no harm for either of them. Additionally, the presence of bioluminescent elytra in *N. chondrocladiae* also points to a mutualistic relationship. Elytra emitting strong luminescence were originally reported by Kirkegaard (2001) in his study describing *Neopolynoe africana* (= *N. chondrocladiae*) and have also been reported and studied for other polynoid species of the genera *Harmothoe* Kinberg, 1856, *Hesperonoe* Chamberlin, 1919 and *Malmgrenia* McIntosh, 1874 (Nicol, 1953; Herrera, 1979; Bassot & Nicolas, 1995; Plyuscheva & Martín, 2009). We found photocytes ventrally on the elytra near the elytrophore scar in *N. chondrocladiae* (Fig. 4A–C), which match the structure of bioluminescent elytra in other polynoids (Nicol, 1953; Bassot & Nicolas, 1995). We showed that the maximum emission wavelength, 525 nm, for the elytra in *N. chondrocladiae* is close to that of purified polynoidin (520 nm), the protein responsible for bioluminescence in polynoids (Nicol, 1953; Bassot & Nicolas, 1995; Plyuscheva & Martín, 2009). In free-living polynoids, the presence of luminescent elytra has been linked to serve as a warning or distracting mechanism (see: Verdes & Gruber, 2017), since elytra detach easily and start flashing upon release, acting as a sacrificial lure and allowing the animal to escape (Nicol, 1953; Plyuscheva & Martín, 2009). Because polynoidin can be activated while the elytra are still attached, and the elytral tubercles act as refractory prisms (Nicol, 1953; Bassot & Nicolas, 1995; Plyuscheva & Martín, 2009), we hypothesize that *N. chondrocladiae* may have co-opted this defence mechanism into a luring mechanism. Light-emitting elytra would attract prey to the vicinity of the host's branches and spicule-rich spheres, increasing the food available for both the sponge and the polynoid. If this hypothesis is true, the relationship between *N. chondrocladiae* and *C. robertballardi*/*C. virgata* would be mutualistic: the polynoid, apart from benefiting from the physical protection provided by the sponge, would also benefit from not having to actively find its prey, while the sponge, apart from benefiting by having a symbiont cleaning its surface and/or dissuading potential predators (see: Mortensen, 2001), would also benefit from more prey items being attracted to the spheres by its symbiont. Bioluminescence, widely considered as the major visual stimulus in the deep sea (Widder, 2013), has proved to act as a visual attractant for zooplankton before. These organisms might use bioluminescence as a visual cue during their search for particles rich in organic material, a cue likely to be detectable in the dark at much greater distances than chemical or mechanical cues (Zarubin *et al.*, 2012). Bioluminescence of marine animals falls within the wavelength range 440–560 nm (Haddock *et al.*, 2010), with examples such as the northern krill mainly being attracted to a wavelength of 530 nm, which makes plausible our hypothesis about *N. chondrocladiae* worms luring potential prey to be captured by its host sponge. In any case, further experiments should be conducted to test this.

CONCLUSIONS

Symbiosis involving marine polychaetes is a growing research field, with new, remarkable examples identified every year. In the majority of the cases, though, our understanding of the biological and ecological functional associations between the species involved is incomplete. By using a multidisciplinary approach (including molecular connectivity, stable isotope analysis, 16S amplicon sequencing, microCT

and other imaging techniques), we have narrowed down the symbiotic relationship between the polychaete *N. chondrocladiae* and its sponge hosts *C. robertballardi* and *C. virgata* to be a mutualistic one. Both the symbiont and the hosts feed on the same organisms, namely the crustaceans and other small marine invertebrates that get trapped, presumably haphazardly, in the spicule-rich spheres of the sponge. We further suggest that the worm might be using its bioluminescent elytra to actively increase the chances of attracting a larger number of potential prey items, thus benefiting both partners. Whether this luring mechanism, never described for polynoids to date, is in fact happening remains to be tested with *in situ* observations or controlled experiments in a laboratory environment.

ACKNOWLEDGEMENTS

This work was supported by the SponGES project (Grant agreement no. 679848) – European Union Framework Programme for Research and Innovation, H2020. We thank Nathan Kenny and Tomasz Goral of the NHMUK's Imaging Facilities for their assistance during confocal microscopy sessions. We also thank Francisco Sánchez, Nathan Kenny, Carlos Leiva, Patricia Álvarez-Campos and the crew of B/O *Ángeles Alvariño* for their help during collection of samples. We also thank, Rachel Przeslawski, Ruth Barnich and an anonymous reviewer, who greatly improved an earlier version of this manuscript. Last, we thank all members of the Riesgo Lab, Martín Taboada and Otilia Moreno, for all the help they provided during the sample processing and writing of the manuscript. ST received funding from the Juan de la Cierva-Incorporación program (IJCI-2017–33116), the Spanish Government and received a fellowship from the Systematics Research Fund (SRF) in 2018. JN was funded by the Spanish National Program Ramón y Cajal (RYC-2015–17809). CDV received funding from the EU Horizon 2020 Marie Sklodowska-Curie 'DeepSym' (grant agreement: 796011). We would like to dedicate this article to the memory of Prof. Hans Tore Rapp, who was a wonderful scientist and person, and an esteemed member of the sponge community. We additionally would like to dedicate our article to George Floyd, brutally killed for no reason while living peacefully in Minneapolis in May 2020.

REFERENCES

Altschul SF, **Gish W**, **Miller W**, **Myers EW**, **Lipman DJ. 1990.** Basic local alignment search tool. *Journal of Molecular Biology* **215:** 403–410.

Apprill A, **Mcnally S**, **Parsons R**, **Weber L. 2015.** Minor revision to V4 region SSU rRNA 806R gene primer greatly increases detection of SAR11 bacterioplankton. *Aquatic Microbial Ecology* **75:** 129–137.

Augener H. 1918. Polychaeta. *Beitrage zur Kenntnis der Meeresfauna Westafrikas* **2:** 67–625

Bassot JM, **Nicolas MT. 1995.** Bioluminescence in scale-worm photosomes: the photoprotein polynoidin is specific for the detection of superoxide radicals. *Histochemistry and Cell Biology* **104:** 199–210.

Bock G, **Fiege D**, **Barnich R. 2010.** Revision of *Hermadion* Kinberg, 1856, with a redescription of *Hermadion magalhaensi* Kinberg, 1856, *Adyte hyalina* (G. O. Sars, 1873) n. comb. and *Neopolynoe acanellae* (Verrill, 1881) n. comb. (Polychaeta: Polynoidae). *Zootaxa* **2554:** 45–61.

Boecklen WJ, **Yarnes CT**, **Cook BA**, **James AC. 2011.** On the use of stable isotopes in trophic ecology. *Annual Review of Ecology, Evolution, and Systematics* **42:** 411–440.

Britayev TA, **Gil J**, **Altuna Á**, **Calvo M**, **Martín D. 2014.** New symbiotic associations involving polynoids (Polychaeta, Polynoidae) from Atlantic waters, with redescriptions of *Parahololepidella greeffi* (Augener, 1918) and *Gorgoniapolynoe caeciliae* (Fauvel, 1913). *Memoirs of Museum Victoria* **71:** 27–43.

Cáceres MD, **Legendre P. 2009.** Associations between species and groups of sites: indices and statistical inference. *Ecology* **90:** 3566–3574.

Callahan BJ, **McMurdie PJ**, **Rosen MJ**, **Han AW**, **Johnson AJA**, **Holmes SP. 2016.** DADA2: high-resolution sample inference from Illumina amplicon data. *Nature Methods* **13:** 581–583.

Chamberlin RV. 1919. Pacific coast Polychaeta collected by Alexander Agassiz. *Bulletin of the Museum of Comparative Zoology* **63:** 251–270

Clement M, **Posada D**, **Crandall K. 2000.** TCS: a computer program to estimate gene genealogies. *Molecular Ecology* **9:** 1657–1659.

Cordiner C. 1793. *Remarkable ruins, and romantic prospects, of north Britain. With ancient monuments, and singular subjects of natural history*. London: Peter Mazell.

Cristobo J, **Ríos P**, **Pomponi S**, **Xavier J. 2015.** A new carnivorous sponge, *Chondrocladia robertballardi* sp. nov. (Porifera: Cladorhizidae) from two north-east Atlantic seamounts. *Journal of the Marine Biological Association of the United Kingdom* **95:** 1345–1352

De Jong MA, **Wahlberg N**, **Van Eijk M**, **Brakefield PM**, **Zwaan BJ. 2011.** Mitochondrial DNA signature for range-wide populations of *Bicyclus anynana* suggests a rapid expansion from recent refugia. *PLoS One* **6:** 1–5.

Dendy A. 1922. Report on the Sigmatotetraxonida collected by H.M.S.'Sealark' in the Indian Ocean. In: Reports of the Percy Sladen Trust Expedition to the Indian Ocean in 1905, Vol. 7. *Transactions of the Linnean Society of London* **18:** 1–164.

Dupont S, **Corre E**, **Li Y**, **Vacelet J**, **Bourguet-Kondracki ML. 2013.** First insights into the microbiome of a carnivorous sponge. *FEMS Microbiology Ecology* **86:** 520–531.

Fauvel P. 1914. Un eunicien énigmatique *Iphitime cuenoti* n. sp. *Archives de Zoologie Expérimentale et Générale* **53:** 34–37.

Fauvel P. 1943. Deux polychètes nouvelles. *Bulletin du Muséum d'Histoire Naturelle, Paris (Série 2)* **15:** 200–202

Folmer O, **Black M**, **Hoeh W**, **Lutz R**, **Vrijenhoek R. 1994.** DNA primers for amplification of mitochondrial cytochrome c oxidase subunit I from diverse metazoan invertebrates. *Molecular Marine Biology and Biotechnology* **3:** 294–299.

Giangrande A. 1997. Polychaete reproductive patterns, life cycles and life histories: an overview. *Oceanograhy and Marine Biology* **35:** 323–386.

González-Pola C, Lavín **A**, **del Rio GD**, **Cabanas JM**, **Ruiz-Villarreal M**, **Somavilla R**, **Rodríguez C**, **González-Nuevo G**, **Nogueira E. 2012.** Capítulo 2. Hidrografía y circulación. In: Bode A, Lavín A, Valdés L, eds. *Cambio climático y oceanográfico en el Atlántico del norte de España*. Madrid: Instituto Español de Oceanografía, Ministerio de Ciencia e Innovación, 69–98.

Haddock SHD, **Moline MA**, **Case JF. 2010.** Bioluminescence in the Sea. *Annual Review of Marine Science* **2:** 443–493.

Hamel JF, **Montgomery EM**, **Barnich R**, **Mercier A. 2015.** Range extension of the deep-sea polychaete worm *Neopolynoe acanellae* in Canada. *Marine Biodiversity Records* **8:** 10–13.

Herrera AA. 1979. Electrophysiology of bioluminescent excitable epithelial cells in a polynoid polychaete worm. *Journal of Comparative Physiology* **129:** 67–78.

Hestetun JT, **Dahle H**, Jørgensen **SL**, **Olsen BR**, **Rapp HT. 2016a.** The microbiome and occurrence of methanotrophy in carnivorous sponges. *Frontiers in Microbiology* **7:** 1781.

Hestetun JT, **Vacelet J**, **Boury-Esnault N**, **Borchiellini C**, **Kelly M**, **Ríos P**, **Cristobo J**, **Rapp HT. 2016b.** The systematics of carnivorous sponges. *Molecular Phylogenetics and Evolution* **94:** 327–345.

Hestetun JT, **Tompkins-Macdonald G**, **Rapp HT. 2017**. A review of carnivorous sponges (Porifera: Cladorhizidae) from the boreal North Atlantic and Arctic. *Zoological Journal of the Linnean Society* **181:** 1–69.

Johnson JY. 1862. Descriptions of two corals from Madeira, belonging to the genera *Primnoa* and *Mopsea*. *Proceedings of the Zoological Society of London* **30:** 245–246

Katoh K, **Standley DM. 2013.** MAFFT Multiple sequence alignment software v.7: improvements in performance and usability. *Molecular Biology and Evolution* **30:** 772–780.

Kearse M, **Moir R**, **Wilson A**, **Stones-Havas S**, **Cheung M**, **Sturrock S**, **Buxton S**, **Cooper A**, **Markowitz S**, **Duran C**, **Thierer T**, **Ashton B**, **Meintjes P**, **Drummond A. 2012.** Geneious Basic: an integrated and extendable desktop software platform for the organization and analysis of sequence data. *Bioinformatics* **28:** 1647–1649.

Kennedy J, **Flemer B**, **Jackson SA**, **Morrissey JP**, **O'Gara F**, **Dobson ADW. 2014.** Evidence of a putative deep sea specific microbiome in marine sponges. *PLoS One* **9:** e91092.

Kinberg JGH. 1856. Nya slägten och arter af Annelider. *Öfversigt af Kongl. Vetenskaps-Akademiens Förhhandlingar Stockholm* **12:** 381–388.

Kirkegaard JB. 2001. Deep-sea polychaetes from north-west Africa, including a description of a new species of *Neopolynoe* (Polynoidae). *Journal of the Marine Biological Association of the United Kingdom* **81:** 391–397.

Kozich JJ, **Westcott SL**, **Baxter NT**, **Highlander SK**, **Schloss PD. 2013.** Development of a dual-index sequencing strategy and curation pipeline for analyzing amplicon sequence data on the miseq illumina sequencing platform. *Applied and Environmental Microbiology* **79:** 5112–5120.

Kübler B, **Barthel D. 1999.** A carnivorous sponge, *Chondrocladia gigantea* (Porifera: Demospongiae), the giant deepsea clubsponge from the Norwegian Trench. *Memoirs-Queensland Museum* **44:** 289–298.

Lattig P, **Muñoz I**, **Martin D**, **Abelló P**, **MacHordom A. 2017.** Comparative phylogeography of two symbiotic dorvilleid polychaetes (*Iphitime cuenoti* and *Ophryotrocha mediterranea*) with contrasting host and bathymetric patterns. *Zoological Journal of the Linnean Society* **179:** 1–22.

Lee WL, **Reiswig HM**, **Austin WC**, **Lundsten L. 2012.** An extraordinary new carnivorous sponge, *Chondrocladia lyra*, in the new subgenus *Symmetrocladia* (Demospongiae, Cladorhizidae), from off of northern California, USA. *Invertebrate Biology* **131:** 259–284.

Leigh JW, **Bryant D. 2015.** Popart : full-feature software for haplotype network construction (S. Nakagawa, ed.). *Methods in Ecology and Evolution* **6:** 1110–1116.

Librado P, **Rozas J. 2009.** DnaSP v.5: a software for comprehensive analysis of DNA polymorphism data. *Bioinformatics* **25:** 1451–1452.

Llave E, **Hernández-Molina FJ**, **Ercilla G**, **Roque C**, **Van Rooij D**, **García M**, **Juan C**, **Mena A**, **Brackenridge R**, **Jané G**, **Stow D**, **Gómez-Ballesteros M. 2015.** Bottom current processes along the Iberian continental margin. *Boletín Geológico y Minero* **126:** 219–256.

Maggs CA, **Castilho R**, **Foltz D**, **Henzler C**, **Jolly MT**, **Kelly J**, **Olsen J**, **Perez KE**, **Stam W**, **Väinölä R**, **Viard F**, **Wares J. 2008.** Evaluating signatures of glacial refugia for North Atlantic benthic marine taxa. *Ecology* **89:** 108–122.

Martín D, **Britayev TA. 1998.** Symbiotic polychaetes: review of known species. *Oceanography and Marine Biology: an Annual Review* **36:** 217–340.

Martín D, **Britayev TA. 2018.** Symbiotic polychaetes revisited: an update of the known species and relationships (1998–2017). *Oceanography and Marine Biology: an Annual Review* **56:** 371–448.

Martín D, **Rosell D**, **Uriz MJ. 1992.** *Harmothöe hyalonemae* sp. nov. (Polychaeta, Polynoidae), an exclusive inhabitant of different Atlanto-Mediterranean species of *Hyalonema* (Porifera, Hexactinellida). *Ophelia* **35:** 169–185.

Martín D, **Nygren A**, **Hjelmstedt P**, **Drake P**, **Gil J. 2015.** On the enigmatic symbiotic polychaete '*Parasyllidea*' *humesi* Pettibone, 1961 (Hesionidae): taxonomy, phylogeny and behaviour. *Zoological Journal of the Linnean Society* **174:** 429–446.

Martín D, **Meca MA**, **Gil J**, **Drake P**, **Nygren A. 2017.** Another brick in the wall: population dynamics of a symbiotic species of *Oxydromus* (Annelida, Hesionidae), described as new based on morphometry. *Contributions to Zoology* **86:** 181–211.

Meca MA, **Drake P**, **Martín D. 2019.** Does polyxenous symbiosis promote sympatric divergence? A morphometric

and phylogeographic approach based on *Oxydromus okupa* (Annelida, Polychaeta, Hesionidae). *Contributions to Zoology* **88:** 173–200.

McIntosh WC. 1874. On the Annelida of the Gulf of St. Lawrence, Canada. *Annals and Magazine of Natural History 13 (4th series) issue 76 part* **34:** 261–270.

McIntosh WC. 1885. Report on the Annelida Polychaeta collected by H.M.S. *Challenger* during the years 1873–1876. *Report on the Scientific Results of the Voyage of H.M.S. Challenger during the years 1873–76. Zoology* **12:** i–xxxvi, 1–554

Molodtsova T, **Budaeva N. 2007.** Modifications of corallum morphology in black corals as an effect of associated fauna. *Bulletin of Marine Science* **81:** 469–479.

Molodtsova TN, **Britayev TA**, **Martín D. 2016.** Cnidarians and their polychaete symbionts. In: *The cnidaria, past, present and future*. Cham: Springer, 387–413.

Mortensen PB. 2001. Aquarium observations on the deep-water coral *Lophelia pertusa* (L., 1758) (Scleractinia) and selected associated invertebrates. *Ophelia* **54:** 83–104.

Nicol JAC. 1953. Luminescence in polynoid worms. *Journal of the Marine Biological Association of the United Kingdom* **32:** 65–84.

Oksanen J, **Blanchet FG**, **Friendly M**, **Kindt R**, **Legendre P**, **Mcglinn D**, **Minchin PR**, **O'Hara RB**, **Simpson GL**, **Solymos P**, **Henry M**, **Stevens H**, **Szoecs E**, **Maintainer HW. 2019.** *Vegan: community ecology package. Ordination methods, diversity analysis and other functions for community and vegetation ecologists*, 05–26. Version 2.5-1. https://CRAN.R-proje ct.org/packa ge=vegan.

Palumbi SR. 1996. Nucleic acids II: the polymerase chain reaction. In: Hillis DM, Mable BK, Moritz C, eds. *Molecular systematics*. Sunderland: Sinauer Associates, 205–247.

Parada AE, **Needham DM**, **Fuhrman JA. 2016.** Every base matters: assessing small subunit rRNA primers for marine microbiomes with mock communities, time series and global field samples. *Environmental Microbiology* **18:** 1403–1414.

Pettibone M. 1969. *Australaugeneria pottsi*, new name for *Polynoe longicirrus* Potts, from the Maldive Islands (Polychaeta: Polynoidae). *Proceedings of the Biological Society of Washington* **82:** 519–524.

Plyuscheva M, **Martín D. 2009.** On the morphology of elytra as luminescent organs in scale-worms (Polychaeta, Polynoidae). *Zoosymposia* **389:** 379–389.

Ravara A, **Cunha MR. 2016.** Two new species of scale worms (Polychaeta: Aphroditiformia) from deep-sea habitats in the Gulf of Cadiz (NE Atlantic). *Zootaxa* **4097:** 442–450.

R Development Core Team. **2019.** *R: a language and environment for statistical computing*. Vienna: R Foundation for Statistical Computing. Available at: http://www.R-project.org/.

Robinson MD, **McCarthy DJ**, **Smyth GK. 2010.** edgeR: a bioconductor package for differential expression analysis of digital gene expression data. *Bioinformatics* **26:** 139–140.

Taboada S, **Serra Silva A**, **Neal L**, **Cristobo J**, **Ríos P**, **Álvarez-Campos P**, **Hestetun JT**, **Koutsouveli V**, **Sherlock E**, **Riesgo A. 2020.** Insights into the symbiotic relationship between scale worms and carnivorous sponges (Cladorhizidae, Chondrocladia). *Deep-Sea Research Part I: Oceanographic Research Papers* **156:** 103191.

Taylor ML, **Roterman CN. 2017.** Invertebrate population genetics across Earth's largest habitat: the deep-sea floor. *Molecular Ecology* **26:** 4872–4896.

Thomas T, **Moitinho-Silva L**, **Lurgi M**, **Björk JR**, **Easson C**, **Astudillo-García C**, **Olson JB**, **Erwin PM**, **López-Legentil S**, **Luter H**, **Chaves-Fonnegra A**, **Costa R**, **Schupp PJ**, **Steindler L**, **Erpenbeck D**, **Gilbert J**, **Knight R**, **Ackermann G**, **Victor Lopez J**, **Taylor MW**, **Thacker RW**, **Montoya JM**, **Hentschel U**, **Webster NS. 2016.** Diversity, structure and convergent evolution of the global sponge microbiome. *Nature Communications* **7:** 11870.

Thomson CW. 1869. On *Holtenia*, a genus and of vitreus dponges. *Proceedings of the Royal Society of London* **18:** 32–35.

Thomson CW. 1873. *The depths of the sea*. London: Macmillan and Co, 527.

Topsent E. 1920. Spongiaires du Musée Zoologique de Strasbourg. Monaxonides. *Bulletin de l'Institut Océanographique, Monaco* **381:** 1–36.

Vacelet J. 2007. Diversity and evolution of deep-sea carnivorous sponges. In: Custódio MR, Hadju GL, Hadju E, Mauricy G, eds. *Porifera research: biodiversity, innovation and sustainability*. Rio de Janeiro: Museu Nacional, 107–115.

Vacelet J, **Boury-Esnault N. 1995.** Carnivorous sponges. *Nature* **373:** 333–334.

Vacelet J, **Duport E. 2004.** Prey capture and digestion in the carnivorous sponge *Asbestopluma hypogea* (Porifera: Demospongiae). *Zoomorphology* **123:** 179–190.

Vander Zanden MJ, **Rasmussen JB. 2001.** Variation in δ^{15}N and δ^{13}C trophic fractionation: implications for aquatic food web studies. *Limnology and Oceanography* **46:** 2061–2066.

Verdes A, **Gruber DF. 2017.** Glowing worms: biological, chemical, and functional diversity of bioluminescent annelids. *Integrative and Comparative Biology* **57:** 18–32.

Verhoeven JTP, **Dufour SC. 2017.** Microbiomes of the Arctic carnivorous sponges *Chondrocladia grandis* and *Cladorhiza oxeata* suggest a specific, but differential involvement of bacterial associates. *Arctic Science* **4:** 186–204.

Verhoeven JTP, **Kavanagh AN**, **Dufour SC. 2017.** Microbiome analysis shows enrichment for specific bacteria in separate anatomical regions of the deep-sea carnivorous sponge *Chondrocladia grandis*. *FEMS Microbiology Ecology* **93:** fiw214.

Verrill AE. 1879. Notice of recent additions to the marine invertebrata of the northeastern coast of America, with descriptions of new genera and species and critical remarks on others. Part I. Annelida, Gephyraea, Nemertina, Nematoda, Polyzoa, Tunicata, Mollusca, Anthozoa, Echinodermata, Porifera. *Proceedings of the United States National Museum* **2:** 165–205.

Weersing K, **Toonen RJ. 2009.** Population genetics, larval dispersal, and connectivity in marine systems. *Marine Ecology Progress Series* **393:** 1–12.

Widder EA. 2013. Bioluminescence. In: Archer S, Djamgoz M, Loew E, Partridge J, Vallerga S, eds. *Adaptive mechanisms in the ecology of vision*. Dordrecht: Kluwer Academic Publishers, 555–581.

Zarubin M, **Belkin S**, **Ionescu M**, **Genin A. 2012.** Bacterial bioluminescence as a lure for marine zooplankton and fish. *Proceedings of the National Academy of Sciences of the USA* **109:** 853–857.

Zhang Y, **Pham NK**, **Zhang H**, **Lin J**, **Lin Q. 2014.** Genetic variations in two seahorse species (*Hippocampus mohnikei* and *Hippocampus trimaculatus*): evidence for middle pleistocene population expansion. *PLoS One* **9:** e105494.

SUPPORTING INFORMATION

Additional Supporting Information may be found in the online version of this article at the publisher's web-site.

Figure S1. Relative abundances of all ASVs aggregated at class level for each sample Classes with relative abundances lower than 0.01% across the dataset were pooled into the category 'low abundant groups'.
Figure S2. Non-metric multidimensional scaling (nMDS) ordination of microbiome similarity among samples of *Chondrocladia robertballardi*, without correction for sampling-site effect.
Figure S3. Bubble plot analysis on the 30 prokaryote families that differed among any pair of tissue type for *Chondrocladia robertballardi.*
Table S1. NCBI and Biosample accession numbers generated in this study. A, 16S and *COI* sequences used for the haplotype networks. B, 16S amplicon sequencing data used for the microbial community analysis. In bold accession numbers generated in the present study.
Table S2. Average relative abundance of prokaryotes grouped by phylum, class and order for the different samples analysed in this study. Environment samples group sediment and water samples.
Table S3. Alpha-diversity statistics for different comparisons.
Table S4. Permanova comparisons for the different samples.
Table S5. Core microbiome by sample (a) and by tissue type (b).
Table S6. Core microbiome by tissue type in *Chondrocladia robertballardi*.
Table S7. Pairwise comparison in bacterial abundance (family level) among tissue samples of *Chondrocladia robertballardi*. Data based on 30 families. Average relative abundance of the 30 families differing among any pair of tissue is also given.